A STUDY OF A PLUG TO COUNTER WIND FORCES

A Thesis

by

NISHANT GUPTA

Submitted to the Office of Graduate and Professional Studies of
Texas A&M University
in partial fulfillment of the requirements for the degree of

MASTER OF SCIENCE

Chair of Committee,	John M. Nichols
Committee Members,	Edelmiro Escamilla
	Kevin T. Glowacki
Head of Department,	Joseph P. Horlen

May 2015

Major Subject: Construction Management

ABSTRACT

The wind loads are one of the greatest environmental threats that exist for a building. Coastal areas close to the equator are especially prone to damage caused by cyclonic wind loads. Historical data shows that there has been a long history of cyclonic activities causing devastating damage to life and property. The legendary storm that saved Japan from invasion about a millennia ago is one such example.

Recent cyclones, such as Typhoon Tip in 1979 and Cyclone Tracy in 1974, have been responsible for causing billions of dollars' worth damage and killing a significant number of people. The maximum gust speed recorded to date, over 200 mph, is capable of destroying a building.

Various building codes and regulations are based on international research that covers the design of buildings for high winds. At higher wind speeds, as seen in cases of cyclones and tornedoes, the external pressure on the buildings shell increases as the square of the wind speed. One of the failure modes for buildings is a catastrophic failure of the window elements in a high-pressure windstorm. The failure creates a resonance, named after Herrmann von Helmholtz, that overloads the roof and walls from the wind pressure and the mass movement of air.

A new device was developed in this research to smoothen the transition from a closed to open state for a buildings opening. The device has a controlled failure of a plug element. The purpose of the research was to develop a test arrangement to generate cyclonic wind pressures inside a box container to test failure load for the plug. The

results show that a plug with a friction joint between the pipe could be used to control the flow of air from the exterior to the interior of a room at a pre-determined pressure inside the box. The system was found to work and able to create a low level of damping to model the Helmholtz resonator. Further research is recommended using different plug samples.

ACKNOWLEDGEMENTS

I would like to convey my sincere thanks and respect to my Chair, Dr. John M. Nichols, and my committee members, Dr. Edelmiro Escamilla and Dr. Kevin T. Glowacki, for their direction and inspiration they have given me to pursue this research and complete it with success.

I would like to thank woodshop supervisor Jim Titus for his guidance and assistance throughout the construction of test apparatus.

Thank you to my parents and other family members for supporting me to pursue my Master's degree at Texas A&M University.

TABLE OF CONTENTS

Page

LIST OF FIGURES

Page

LIST OF TABLES

Page

CHAPTER I

INTRODUCTION

Background

Wind loads are one of the most damaging forces to buildings, especially in coastal and tropical regions (J. D. Holmes, 1994). Unlike earthquakes, snow and flood loads, wind loads can occur at any location on the world. They do not discriminate between rich and poor. The eastern coast of the United States and the northern coast of Australia are susceptible to extreme wind events caused by cyclonic wind activity. A failure mode in these storms is a sudden loss of a window (J.D. Holmes, 2001).

The purpose of this study is to investigate the sudden failure of a sealed opening in a timber box. The timber box is used to represent the typical room in a typical house on the eastern coast of the United States, which is subjected to a cyclonic force wind event.

A sudden window failure allows the higher-pressure external air to rush into the internal space. This inflow can cause the development of a Helmholtzian resonance with the air stream. As with all resonance functions, the level of damping has a significant impact on the resultant airflows. In a fluid flow, such as is occurring in this type of failure the size of the opening compared to the volume of the room is a critical factor, the smaller the ratio between the two numbers the higher the damping level. In this study, the interest is in a very high damping level resulting from a small opening in the wall that suddenly fails.

This thesis outlines the research problem, review of the literature to understand the scope of the problem, the problem statement and the hypothesis, the study method, results and conclusions.

Problem statement

A one cubic meter box is used to represent the typical room in a small house. A small 30 millimeter tube and a friction plug represent a window. A wind pressure equivalent to that generated in a cyclonic wind event fails the plug in the tube. The research work is to study pressure at the point of the friction failure of a 30 mm plug in a tube and the pressure drop with time in the box.

Hypothesis

The following hypothesis will be tested for the study:

The failure of the pressure plug will equalize internal and external pressures for the box in a highly damped manner.

Limitations

The study limitations are:

1. The box is assumed to represent a small room in a small house.
2. Air pressure inside the box will represent a static point in a cyclonic wind event.
3. The pressure transducers can adequately represent the change in pressure with time.

4. The plug used in the study is made from TPE Ninja flex Filament, a material dominantly used for 3d printing, and the leakage rate for the plug is acceptable.

CHAPTER II

LITERATURE REVIEW

Introduction

This chapter outlines the review of literature for this research study. The topics presented in the review are the critical design storms, wind data statistics, vulnerability and risk, wind data, wind scales and Helmholtzian resonance.

Two areas of interest occur with this research, the first is Australia and the second is the United States. J.D. Holmes (2001) studied this problem since the catastrophic cyclone that struck Darwin, Northern Territory, Australia on Christmas Day in 1974. This event and subsequent research has significantly improved the understanding of the failure mode for houses and small commercial buildings in extreme events. The last decade in the United States has seen a number of major hurricanes that damaged infrastructure and claimed lives. These events led to changes in the major US wind loading code to reflect the improved understanding of wind loads and actions (American Society of Civil Engineers & Structural Engineering Institute, 2005, 2010). The critical question is to determine the design storms for the purposes of code development.

Definitions

The definitions used in this research work are:

∂A cross-sectional area

a constant used in the extreme value distribution analysis

γ	ratio of the specific heats of the fluid, which for air at 20 C is 1.4
C	coefficient for the pressure equation
C_{pe}	Pressure coefficient external
C_{pi}	Pressure coefficient internal
F_U	extreme value distribution function for wind
k	constant used in the extreme value distribution analysis
ρ	air density
P	wind pressure
U	clear stream wind velocity for extreme value distribution measured at 10 m height
V	wind velocity

Critical design storms

The codes and regulation published by various government and international agencies are subject to change at regular intervals, typically ranging from three to ten years. Every few years, these new codes provide changes required to cater for the environmental challenges and wind events, such as storms or cyclones. A major wind storm on Barrow Island, Western Australia, in the mid 1990s has shown the extreme values that can strike a residential community and clearly had an impact on the perception as to the likely upper ranges of these wind events.

Three critical storms show in detail the issues and threats associated with storms. Cyclone Tracy occurred in Northern Australia in 1974 is an interesting reference point for data analysis of wind speeds. Figure 1 shows an aerial view of the storm.

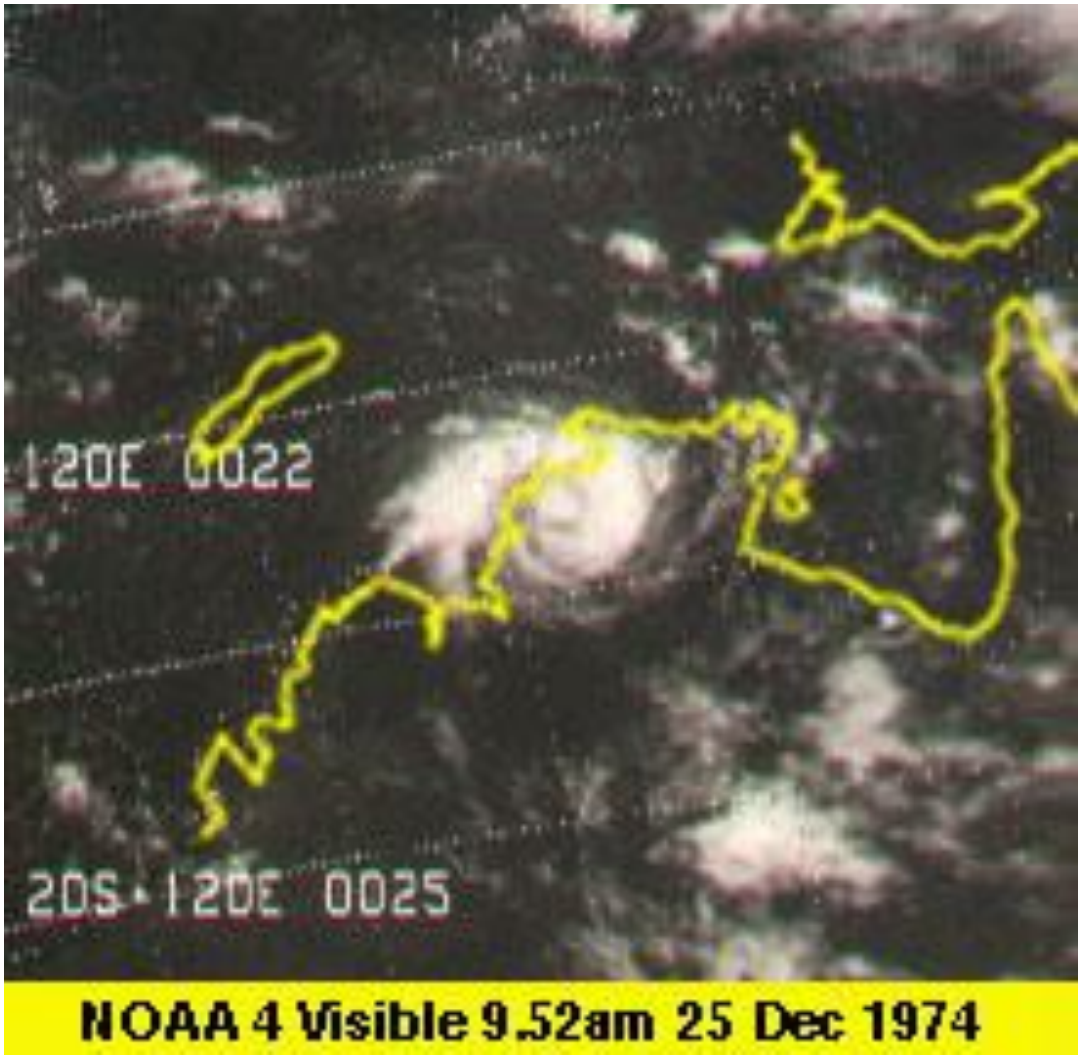

Figure 1. Cyclone Tracy (from NOAA, 1974)

Cyclone Tracy was responsible for major destruction and population reallocation. The cyclone had a maximum gust speed of 135 miles per hour with a wind center radius of 18 miles. It was classified in category 3 according to the Saffir-Simpson Hurricane Wind Scale. This storm should not have caused this level of damage; the explanation is the failure of windows led to catastrophic roof failures and a massive building loss.

In the year 2008, Tropical Storm Marco struck Mexico. It is the most compact hurricane on record to this date. The cyclone had a maximum gust speed of 65 miles per hour and a wind center radius of 12 miles. Figure 2 shows the aerial view of the storm.

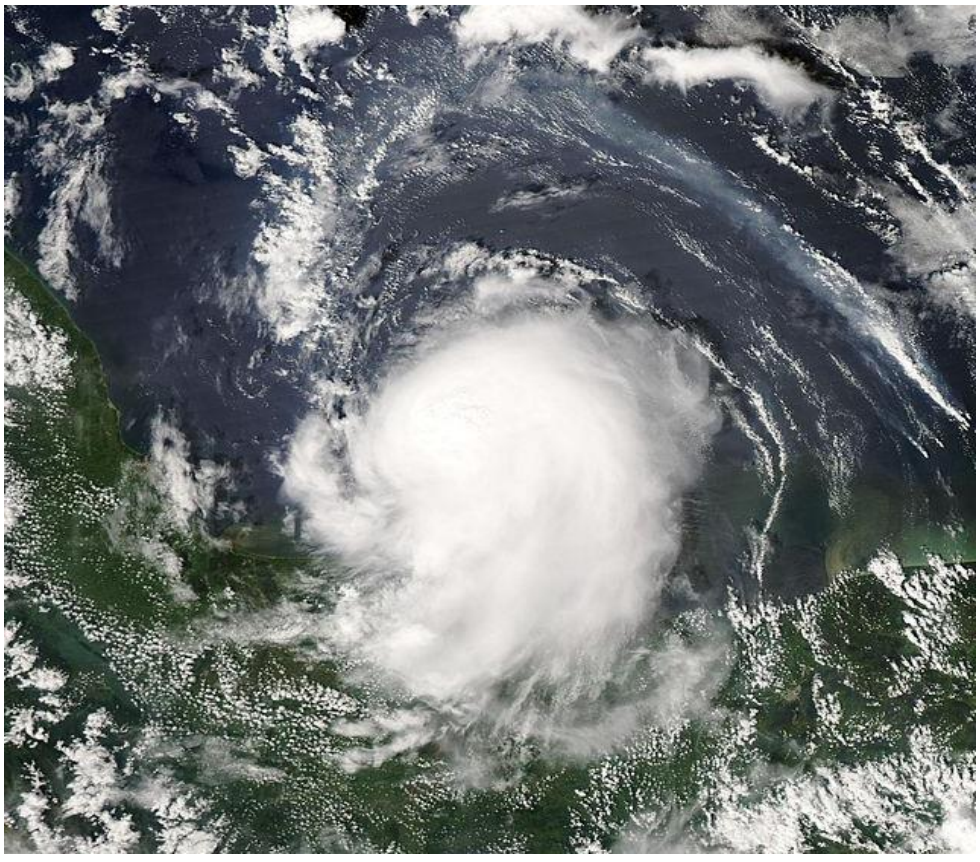

Figure 2. Tropical Storm Marco (from NHC, 2009)

The relative scale of the storm is visible in the figure, compared to Typhoon Tip is it tiny.

Typhoon Tip was the largest and strongest cyclone ever recorded in human history. The cyclone occurred in 1979 and affected regions of Guam, Japan and the Soviet Union. The cyclone had a maximum gust speed of 65 miles per hour and a wind center radius of 1380 miles. Figure 3 shows aerial view of the storm.

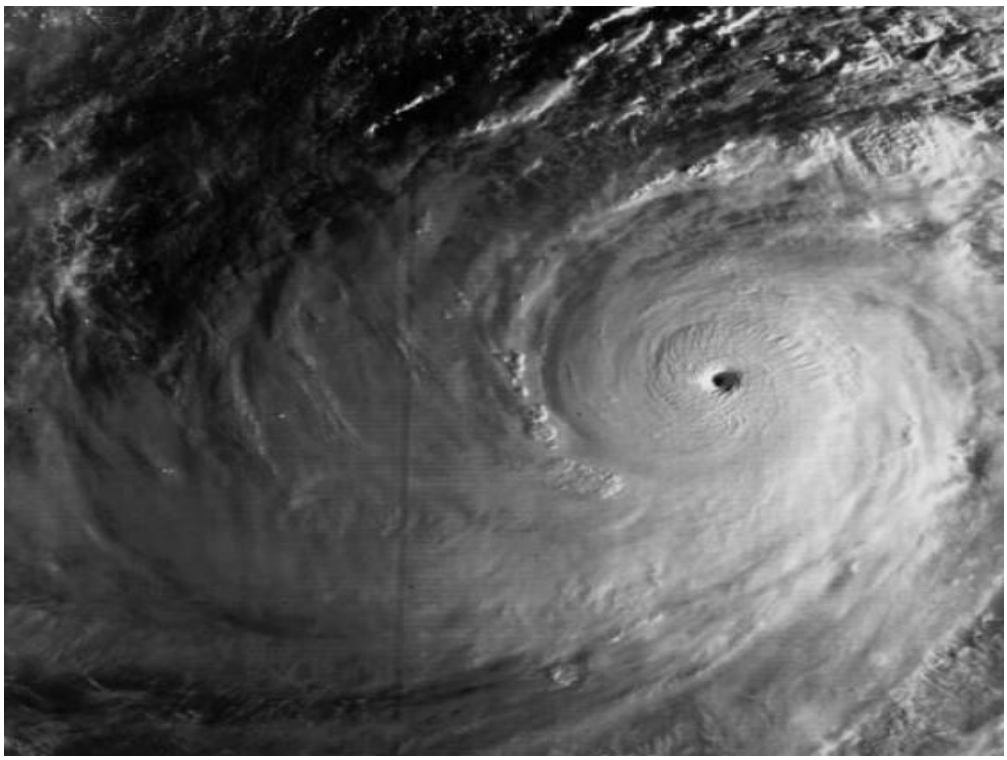

Figure 3. Typhoon Tip – 1979 (from NOAA 1979)

The track of the storm can be seen in Figure 4. The colored dots on the picture show the storm intensity. The torrential rain on Japan resulted in the failure of a detention basin and the deaths of some US marines.

Figure 4. Typhoon Tip Track showing the – 1979 Storm (from NOAA, 1979)

The real problem is the data records. The last few decades have seen a vast improvement in the collection of storm and wind data from satellites, surface buoys and aircraft flights during storms. The data collection still exists on essentially a linear time scale, whereas wind speed is measured on a much longer span logarithmic scale. This observation means that data from the entire world needs to be reviewed in the development of standards and not just the use of a local parochial view of the likely wind speeds. Wind analysis uses an extreme value distribution to look at this data.

Generalized extreme value distribution

The generalized extreme value distribution estimates the maximum or minimum number of weather entries (Jenkinson, 1955). These weather entries could be wind speed. The equation governing the distribution is shown in.

$$F_U(U) = \exp(-[1-k(U-u)/a]^{\frac{1}{k}}) \tag{1}$$

On the basis of k value from equation (1), three distributions types are designated mathematically. Type III if $k < 0$, Type II if k is > 0 and Type I if k approaches 0.

The equation form for Type 1 is shown in equation

$$F_U(U) = \exp\{-\exp[-(U-u)/a]\} \tag{2}$$

A sample using the generalized extreme value distribution method is provided by J.D. Holmes (2001) for the wind speed in Victoria, Australia, during the time period 1952-1998. The sample distribution can be seen in Figure 5.

The high peak value of 42.2 meters per second in the year 1998 is of special interest. The recurrence intervals of a certain wind speed can be determined from Figure 6. The form in which the data is depicted in Figure 6 uses Gringorton method. The Gringorton method, as explained in J.D. Holmes (2001), is a simple transformation of logarithmic based domain to a linear domain.

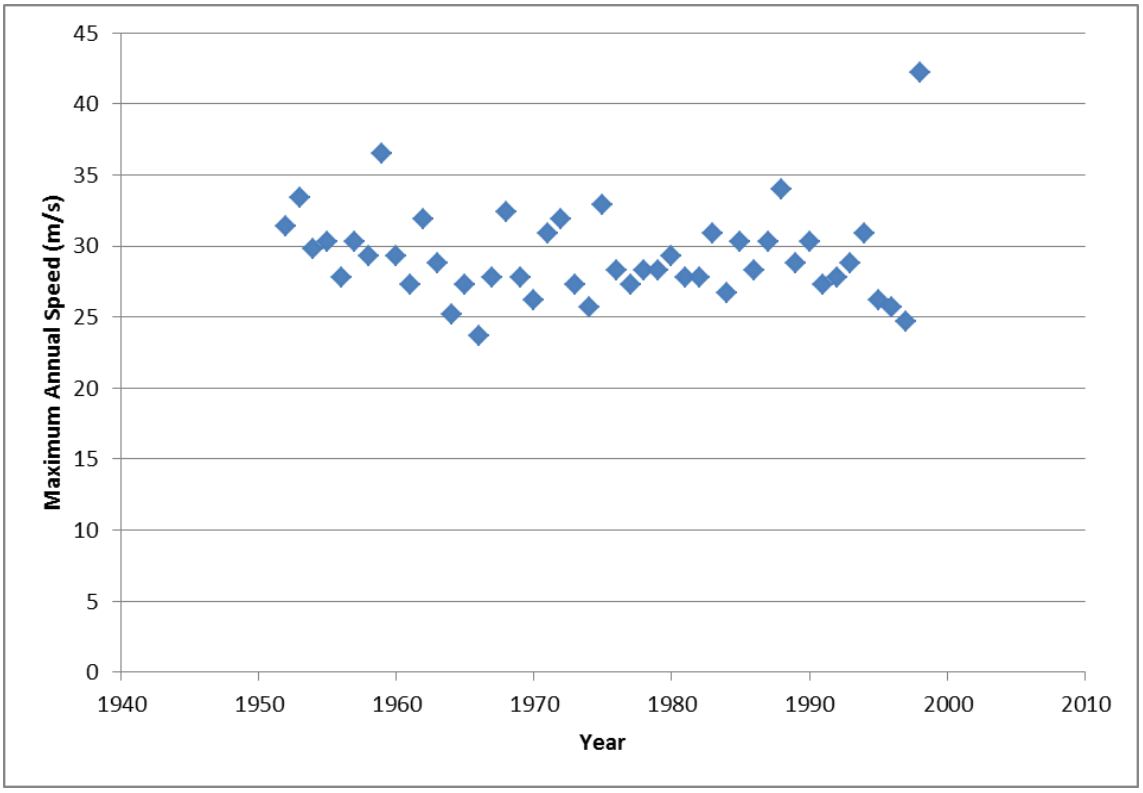

Figure 5. Annual maximum gust speed - East sale 1952 – 1998 (after Holmes, 2001)

Figure 6 provides a means to estimate the return periods of different wind speeds. A five percent occurrence rate in a period of fifty years is the typically used return period for design purposes. Risk is determined to some degree at a political level, the level of risk acceptable to the general population appears to be dropping as the community gains a better understanding of the options and costs associated with risk (Hall & Wiggins, 2000).

The critical aspect for design is to determine the vulnerability of the housing and other buildings to extreme wind loads.

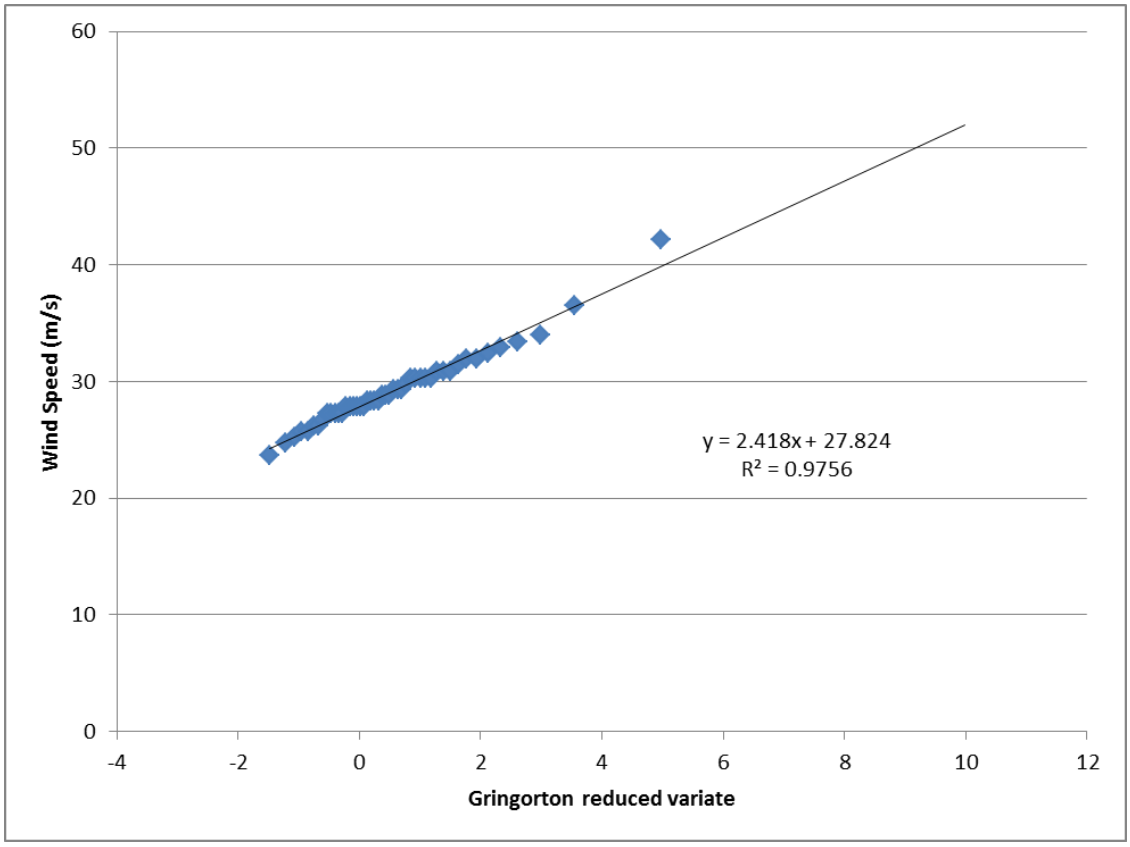

Figure 6. Annual maximum gust speed - East sale 1952 – 1998

Vulnerability to wind loads

Structures designed in recent times are usually more capable of sustaining high wind loads compared to older houses (J. Ginger, Henderson, Edwards, & Holmes, 2010). The buildings are constructed, using locally prevalent building codes. Due to flaws in construction and design or noncompliance of pertinent building codes, buildings are subjected to hazards related to wind. The effect of wind loads can be greatly disastrous on old construction as observed in post windstorm damage surveys and data collected from the insurance industry (J. Ginger et al., 2010). These wind loads are capable of

causing serious damages to buildings. Windstorms, hurricane, cyclones and other severe wind loads lay a lot of pressure on the walls and the roof of the buildings.

The Saffir-Simpson Hurricane Wind Scale is a categorization for the hurricanes intensity. This categorization is done on a scale of 1 to 5, which states the expected damage based of the wind speed. Table **1** shows the scale broken down by winds speeds.

Table 1.

Saffir-Simpson Hurricane Wind Scale

Category	Wind Speed (mph)	Damage
1	74 - 95	very dangerous winds will produce some damage
2	96 - 110	dangerous winds will cause extensive damage
3	111 - 129	devastating damage will occur
4	130 - 156	catastrophic damage will occur
5	> 156	catastrophic damage will occur

Wind causes loads that are external and internal. These loads, measured normal to the walls and roof, may add or subtract depending on wind direction and velocity. The issue is to determine a reasonable design wind speed and determine an acceptable range of loading coefficients for the different building elements.

The data collected from post windstorm damage assessments can help to estimate the expected damage for various types of building types and to develop prevention strategies. Over the years, the researchers have developed software programs and designs to assess and mitigate the risks associated with wind loads. It has been estimated that most of the damage occur due to failure of key components, i.e., connections (Wehner, Ginger, Holmes, Sandland, & Edwards, 2010).

Coastal regions and tropical regions are more vulnerable to wind loads due to extreme tropical cyclones (J. D. Holmes, 1994). The study of wind related damage on tropical houses can be of great use since there is abundant data and the results can be applied to non-tropical housing (J. D. Holmes, 1994).

Research conducted by J.D. Ginger and Holmes (2003) on wind loads on gable ended low rise buildings has found that the effects of oblique approach winds generates substantial design wind load effects on the frames near gable end. Research has been conducted to determine effects on the wind pressure distributions due to the length to span aspect ratio. It has been found that there is a significant increase in the negative pressure coefficient on the roof and the leeward wall with the increase in the aspect ratio in low rise buildings (J. D. Holmes, 1994).

The application of the different findings from other parts of the world requires an understanding of the common elements in all windstorm analysis. The key areas used for this work are Australia and the United States.

Australian wind data

Figure 7 shows the wind regions in Australia from the Australian Standard AS 1170.2.

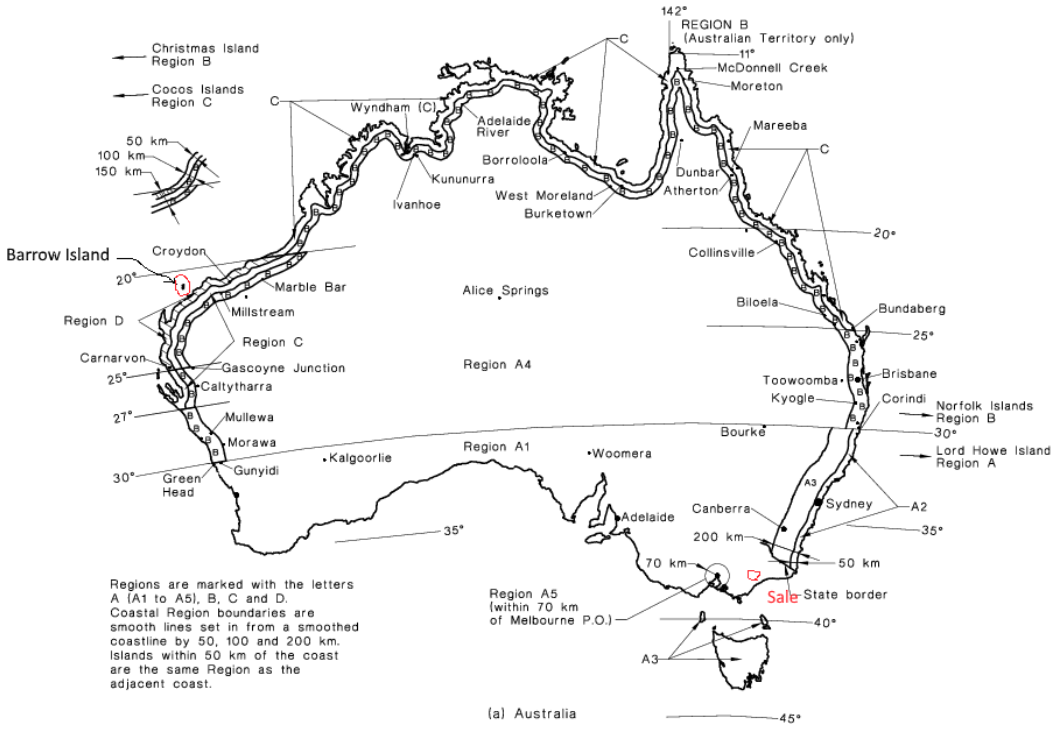

Figure 7. Australian Standard 1170 Part 2 wind regions (from AS 1170)

The map is shown to highlight the location of a non-cyclonic region Sale, which was used as the example of the previous wind speed analysis. Sale is located at the

southern coast of Australia relative to the 40th latitude. The wind data analysis for Sale from the data provided in Holmes (2001) is found to be consistent with the recommended values for the central Australia.

United States wind data

Figure 8 shows the wind speeds in United States from the International code council (2012).

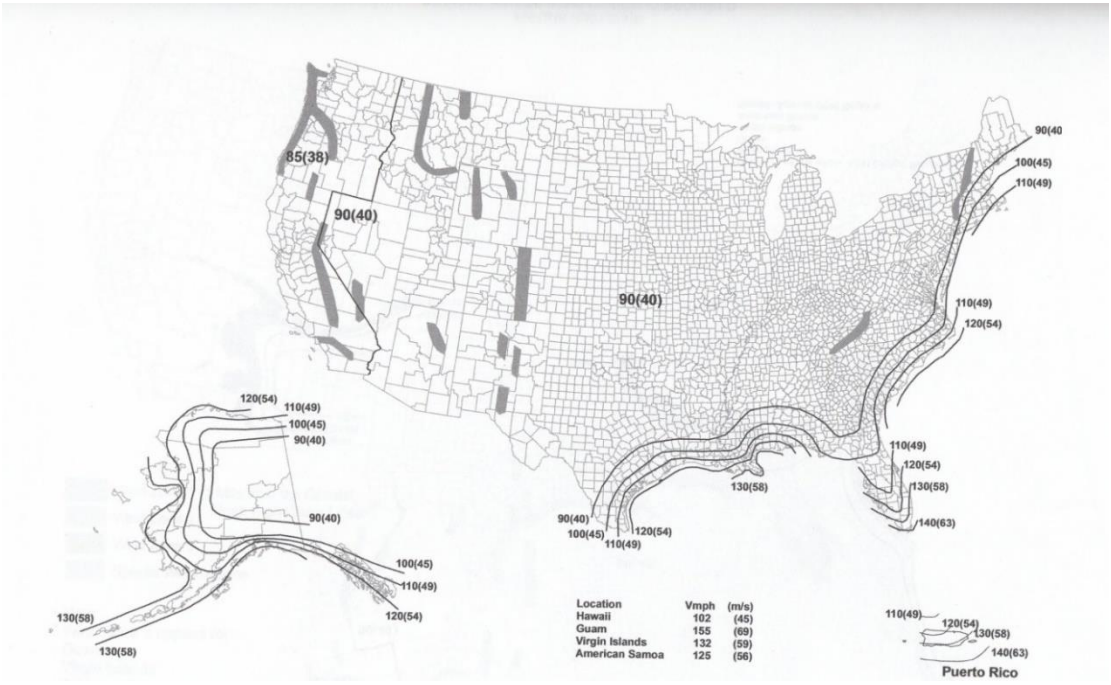

Figure 8. US basic wind speeds (from ICC 2012)

Base wind speed

Hence, it can be concluded that the base value of wind speed for design purposes in Australia should be 40 meters per second. This limit is the lower design limit, which

can be used as the bare minimum for all design codes pertinent to Australia. The wind data of the US was found to be consistent with the Australian wind data. The difference between United States and Australia is the large population settlement on the coastal regions of United States exposing a huge population to disastrous cyclonic events.

The basic wind speed for the central region of United States is 40 meters per second, which is consistent with the base wind speed for Australia. The highest base wind speed in United States was at the tip of Florida a 62.5 m/s.

Mt. Washington and Burrow Island experienced the highest recorded wind speeds under standard measurement conditions. Mt. Washington observatory researchers recorded a peak wind speed of 105 meters per second.

Barrow Island recorded a peak wind speed of 115 meters per second. For engineering and design purposes, Burrow Island is more significant as its inhabitants are general population, not researchers.

Wind storm scale

The Saffir-Simpson Hurricane Wind Scale has five categories from one to five, five being the highest. The 5^{th} category has a lower limit of 70 meters per second but does not have an upper limit for this category. This scale is not fit for use in engineering or design purposes, although it can be used for public information purposes. The incremental change in scale categories of the Saffer- Simpson Hurricane Wind Scale can be seen in Figure 9.

The changes in the scale categories are not symmetric and cannot be effectively used for design purposes. Given the unsymmetrical nature of the Saffer- Simpson Hurricane Wind Scale, a different scale with consistent increment may be more appropriate for design purposes.

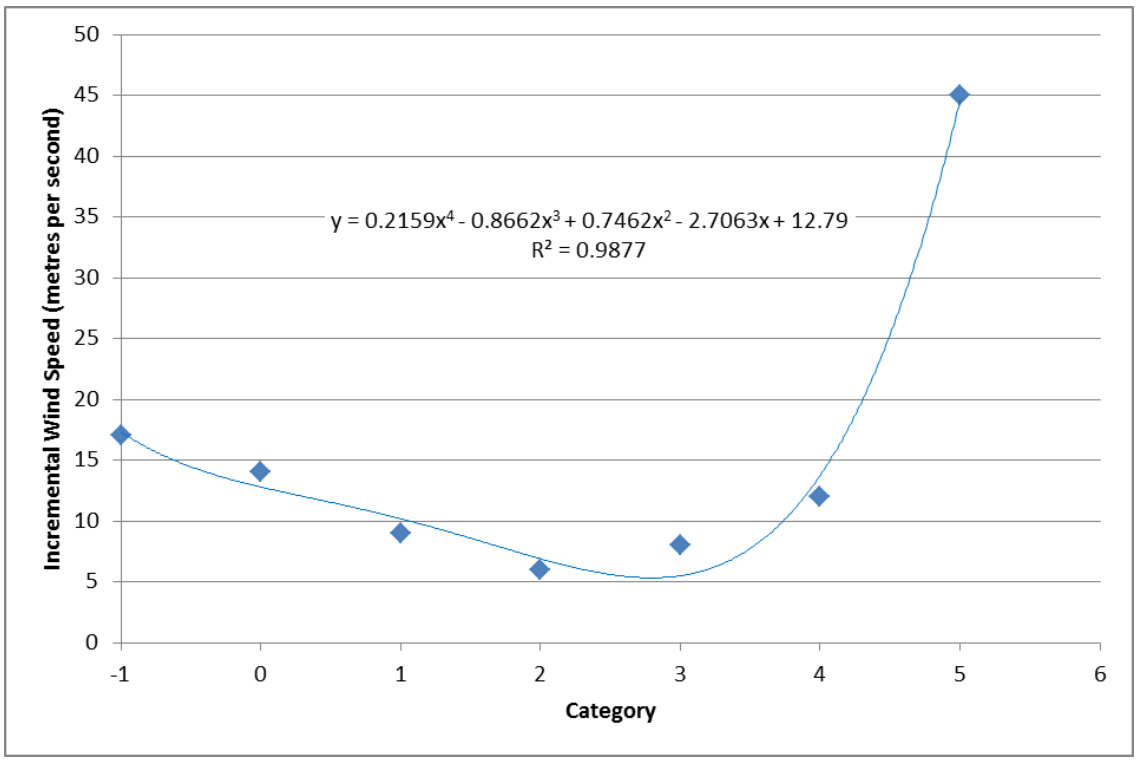

Figure 9. Incremental category change in wind speed

Dominant openings and internal pressures

Internal wind pressure in an enclosed building are typically not as high when compared to the external pressures, but the failure of doors or windows may create dominant openings which can lead to large internal pressure (J.D. Ginger, Holmes, & Kim, 2010).

Dominant openings can either be formed by windborne debris or be left open accidentally. In strong winds, internal pressure coupled with the external pressure acting in the same direction can have a damaging effects on the building (J. D. Ginger, Holmes, & Kopp, 2008).

Internal wind pressure in a building is dependent on various factors such as type, orientation, size of the openings and volume of the building (J. D. Holmes & Ginger, 2009). In a case study on a building with dominant opening, conducted by J. Holmes and Ginger (2012), it was found that dominant openings can produce high positive peak pressures which in combination with external pressures acting on the roof can generate high net pressures resulting in roof failures. This is caused by Helmholtzian resonance.

Helmholtz resonator model

J. D. Ginger et al. (2008) studied the fluctuations in internal pressure based on the Helmholtz resonator model and the existing proposals for peak internal pressure codification to develop a simplified coding which can be used in design codes and standards.

A Helmholtz resonator is a well-known device in acoustic analysis. The resonator was originally applied in the situation where the external pressures were caused by acoustic sources, although it can be applied to cases where the external pressure is caused by wind forces. The acoustic resonator is usually made of brass and was originally installed in amphitheaters to improve the acoustics.

The resonator equation essentially describes the response of small volumes to the external pressure (J.D. Holmes, 2001). In the study of internal air pressures, it is assumed that a defined air "slug" moves in and out of a dominant opening in response to the changes in the external air pressure. Figure 10 shows the Helmholtz resonator model for internal pressure fluctuations with one dominant opening.

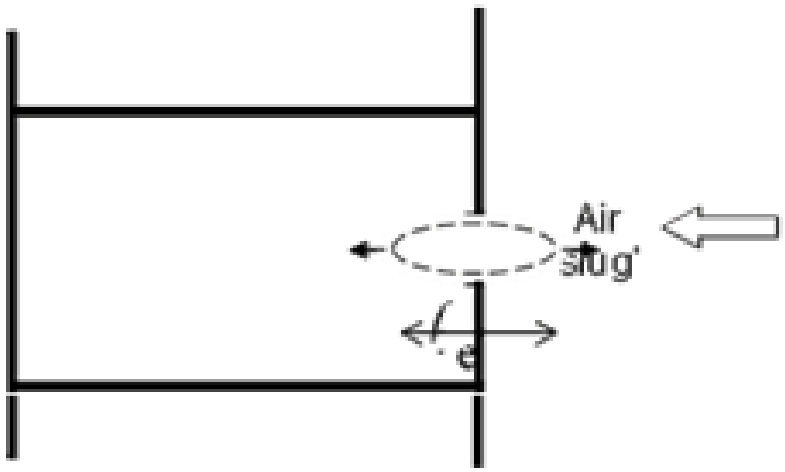

Figure 10. Helmholtz resonator model (from Holmes, 2001)

The differential movement of the air slug is derived in equation (3):

$$\rho A l_e \ddot{x} + \frac{\rho A}{2K^2}\,\dot{x}|\dot{x}| + \frac{np_0}{V_0}\,x = \Delta p_e A \qquad (3)$$

The equation calculates the displacement of the air slug form its original position. The first term on the left hand side of the equation represents the mass of the air slug, the second is associated with the loss of energy at the orifice and the third term is the stiffness presented by the air pressure already in the internal volume. J.D. Holmes (2001) provides the key steps in the development and outline of the solution of this standard

equation. The governing differential equation in terms of pressure coefficients for internal pressures with a one dominant opening can be seen in equation (4).

$$\frac{\rho l_e V}{n p_0 A}\ddot{C}_{pi} + \left[\frac{\rho V \bar{U}_h}{2nkApp_0}\right]^2 \dot{C}_{pi}|\dot{C}_{pi}| + C_{pi} = C_{pe} \quad (4)$$

The first term and the second term represent inertial effects and the damping caused by the frictional losses in the flow through the orifice respectively. C_{pi} *and* C_{pe} represents the internal pressure coefficients. The Helmholtz frequency equation is:

$$f_H = \frac{1}{2\pi}\sqrt{\frac{nAp_0}{\rho l_e V}} \quad (5)$$

It can be observed from the Helmholtz frequency equation, that the ratio of the opening area to the internal volume is inversely proportional to the damping effect.

Orifice analysis

The assumption made by these researchers in looking at the failure of a window is that the equation for the air flow into a building from a square open window is the orifice equation. The orifice equation is a direct equation with a constant linking the flow and the area of the window. The orifice co-efficient used is in the range of 0.6 to 0.7.

At this stage, this can be considered a reasonable estimate although further confirmation by experimental research is suggested for this assumption.

Characteristic length

Helmholtz resonance occurs when a slug of air vibrates in and out of a building through an opening. The model used for the American Society of Civil Engineers and

Structural Engineering Institute (2010) is an assumption that a four square foot window is effectively sealed. A reasonable assumption is a volume of 100 cubic meters for a sample room.

A characteristic length value, termed λ, can be developed based on equation (6)

$$\lambda = \frac{V}{A} \tag{6}$$

Where A is the opening area and V is the room volume. The American Society of Civil Engineers and Structural Engineering Institute (2010) assumption for the nominal volume provides a λ of 270.

Summary

The concept of the Helmholtz resonator as one of the causes of building failure has developed since Cyclone Tracy in 1974. This study looks at a highly damped model to avoid resonance.

CHAPTER III

EXPERIMENTAL PROCEDURES

Introduction

This chapter outlines the experimental procedures used for the work. The work is based on a highly damped system that limits the Helmholtz equation to a non-harmonic form.

The diameter of the pipe used for the outlet is 30 mm and the volume of the box is one cubic meters. The λ value is 35, which is less than the range adopted by American Society of Civil Engineers and Structural Engineering Institute (2010) for effectively sealed. The wind velocity limits established from Barrow Island is 250 miles per hour. This wind speed sets the upper limit to this study. The lower limit is the 40 meters per second used in the interior of Australia and the United States. The pressures were created in closed conditions and were aimed to emulate wind loads acting on residential buildings during windy weather. The equivalent wind pressure of a 250 mph windstorm can be produced by the high pressure air system

A plug has been designed to fit snugly into the outlet pipe and provide a friction seal. The objective of this research is to test and measure the friction resistance of a circular plug having a diameter of 30mm against cyclonic wind pressures. The secondary objective is to determine if the system acts in a highly damped manner.

Experimental methods

Introduction

Figure 11 shows the test system layout comprising of all the major elements of the experiment.

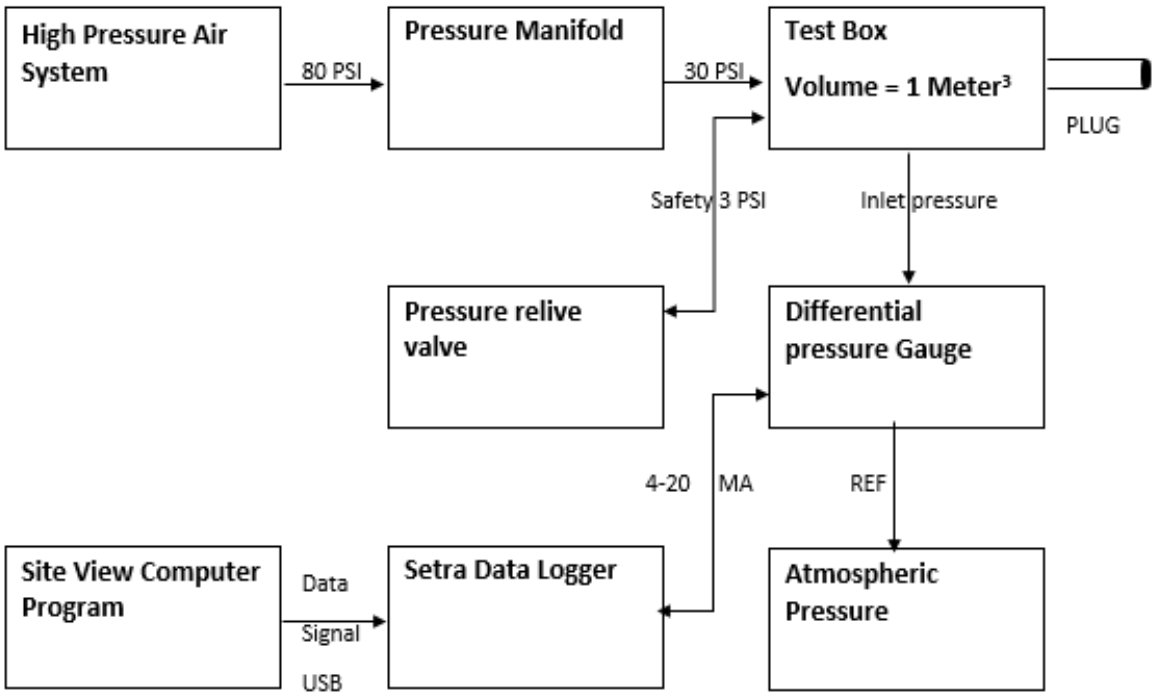

Figure 11. Test system layout for the experiment

Equipment

The apparatus used in this experimental work is:

- High Pressure Air System
- Pressure Gauge

- Test Box
- Differential Pressure Transducer
- Data Collection Device

The details of the equipment and the experimental devices developed for this work are outlined in these sections of the thesis.

High Pressure Air System

A supply of compressed air at high pressure was used for the test box. The high pressure air system is a Model 2-475 compressor manufactured by Ingersoll Rand. The system is capable of supplying air at the rate of 24 cubic ft. per minute at 90 psi.

Figure 12 shows the air pressure system. The high pressure air is used to charge the box with air equivalent to a maximum of 0.8 psi, which is 115 psf.

Figure 12. Air compressor

The inlet air is fed to a high range pressure gauge.

High Range Pressure Gauge

Figure 13 shows the high range pressure gauge, 0-160 psi on the left hand side of the picture,

Figure 13. Pressure gauges and needle valves

The inlet air pressure was set to a maximum of 110 psi.

Needle Valve

A needle valve was used to introduce a consistent loss into the system. This valve took the 110 psi air and reduced the pressure to about 30 to 40 psi. The secondary system limit is the large volume and the flexibility of the timber box which responds slowly to the applied air pressure in terms of internal pressure changes.

Low Pressure Gauge

A pressure gauge with a capacity of 30 to 40 psi was used to monitor the inlet pressure into the test box.

Test Box

A test box, or box enclosed on all six sides having an inside volume of 1 meter cube was constructed to represent a room in a house. Medium density fiberboard of thickness 19 mm was used to construct the test box. Figure 13 shows the top of the completed box.

To begin, all the dimensions were determined. The dimensions for different sides of the box are shown in Figure 14. Three different sizes for the sides were determined and were named panel A, panel B and panel C. Two pieces of each type of panel are required for to form the six sides of the box.

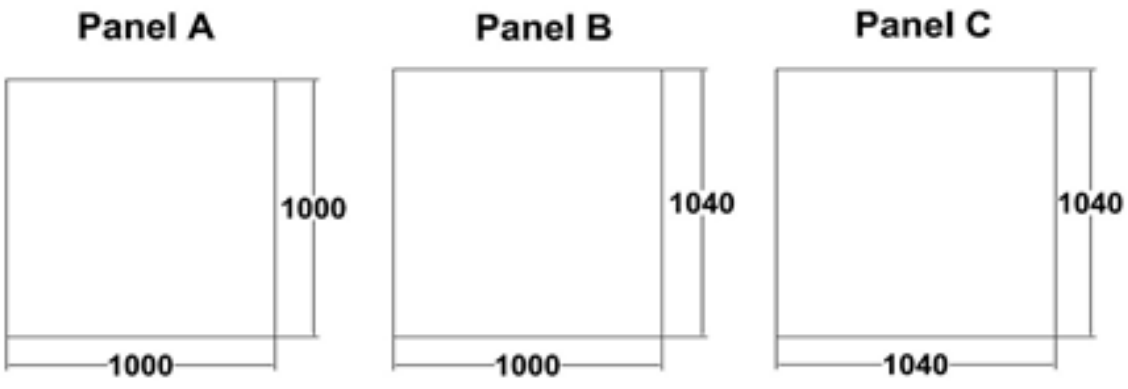

Figure 14. Dimensions of panel A, panel B and panel C

A three dimensional figure of the box was created using AutoCAD computer programme. Figure 15 & Figure 16 shows the top view and isometric view of the model. The MDF sheets of 49”x 97” were reduced to workable size sheets using a panel saw. Figure 17 shows the panel saw used to cut the medium density fiberboard (MDF).

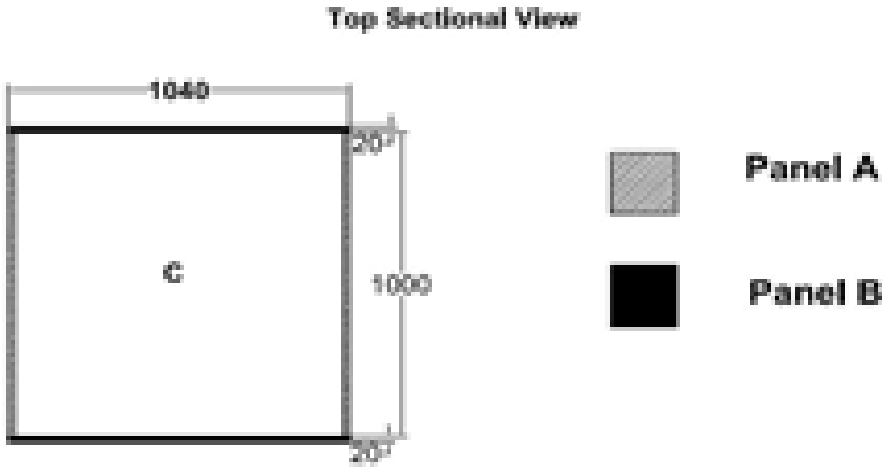

Figure 15. Top sectional view of test box

After measuring and marking the workable size sections of MDF, cuts were made using table saw. The panels were marked as panel A (1000 mm X 1000 mm), panel B (1000 mm x 1040 mm), and panel C (1040 mm x 1040 mm) before the cuts were made through the table saw.

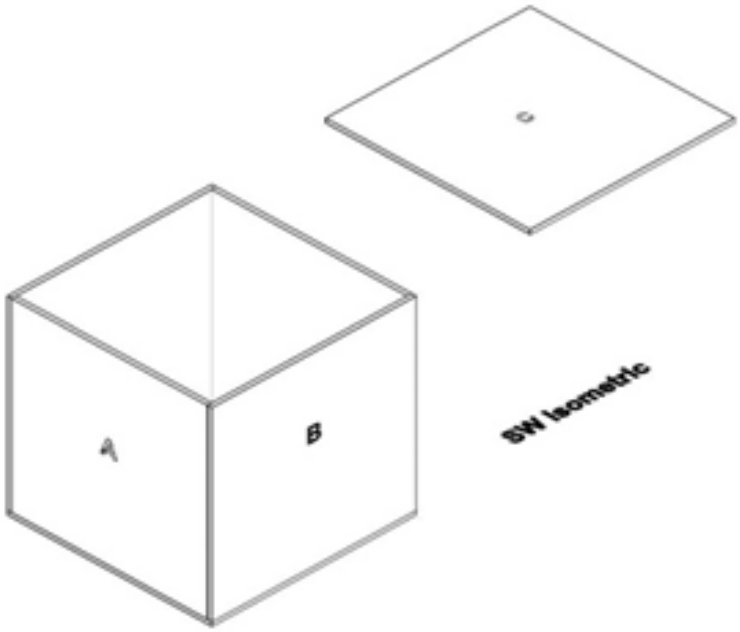

Figure 16. Isometric view of the test box

Figure 17. Panel saw used to cut the panels

For some difficult cuts, a jaw stand was used to provide support to the panel. Figure 18 & Figure 19 shows panel C being cut using the table saw and the marked panels A, B and C.

Figure 18. One of the panels is trimmed using the table saw

Figure 20 shows the jaw stand being used to provide support during a cut. MDF is permeable in nature and will not be air tight under high pressures. For the purposes of this experiment, the test box is required to be air tight. To overcome the permeability factor of the MDF sheets, the panels are coated with a combination of denatured alcohol and epoxy. Equal quantities of epoxy and denatured alcohol are mixed to make the coating solution. Epoxy serves as the anti-permeability agent and denatured alcohol increases the applicability of the solution.

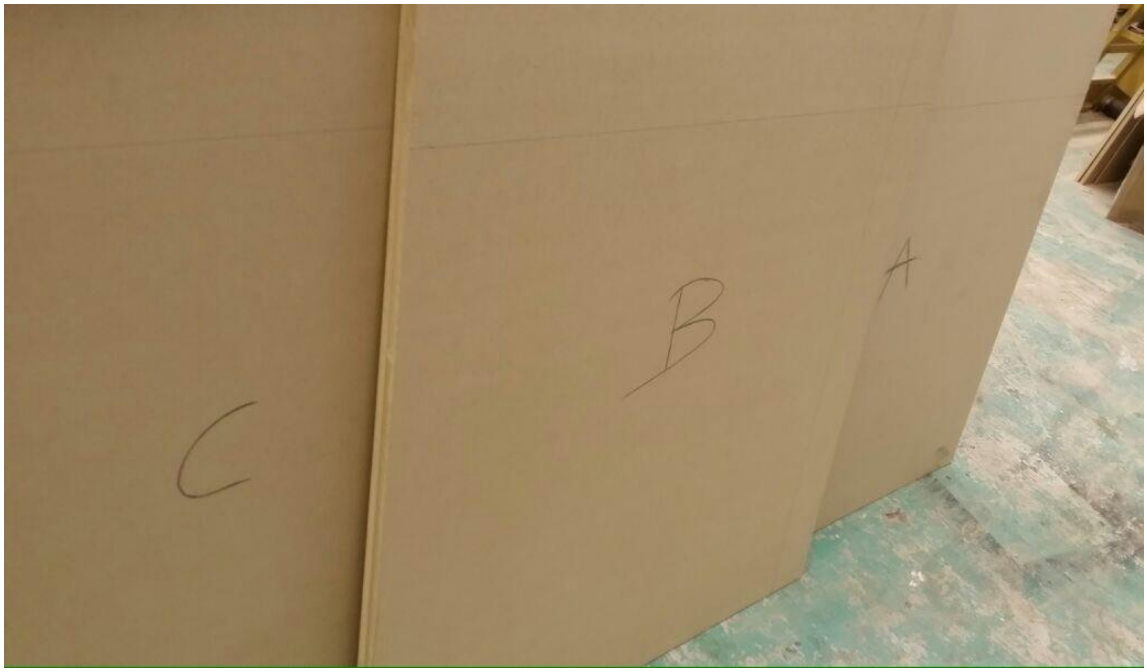

Figure 19. Marked panels A, B and C

Figure 20. Jaw Stand to provide support to the panel

Figure 21 shows a newly coated panel A.

Figure 21. Panel A coated with a mixture of epoxy and denatured alcohol

The precision of dimensions of the text box are important to the experiment. Due to the relatively large size of the box it is difficult to install the box correctly. The panel sides are first erected and checked for dimension correctness before final installation. Figure 22 shows the five sides of the box being held by a clamp.

Figure 22. Test box panels before installation

The edges of the panel are glued with a mixture of epoxy and wood dust and attached together. Both sides of panel C and one side of panel B was kept 40 mm larger that the desired side dimension of one meter. The additional 40 mm was kept to account for the 19 mm thickness of the MDF on both sides. The remaining 1 mm on each side was accounted by the epoxy and wood dust mixture. Figure 23 shows the gluing mixture being prepared and Figure 24 shows the test box of which five sides have been glued.

Figure 23. Epoxy and wood dust being mixed

Figure 24. Test box with five sides installed

Due to the relatively large size of the box, the installation of the six side of the box required the box to be demounted from the platform. To provide initial stability, the edges of the box were fastened using a nail gun. Figure 25 shows the edges being fastened using the nail gun.

Figure 25. Edges of test box being fastened using nail gun

A hole for the later installation of pressure valve was made and the sixth side of the box was glued. Figure 26 shows the installed test box.

Figure 26. Installed test box

Table 2 shows the materials and equipment used for experimental work.

Table 2.

Materials and equipment's used for the experiment

Materials used in Experiment		Equipment used in Experiment	
Material	Comment	Tool	Comment
Fibre Board	19 mm MDF	Panel Saw	Cut MDF
Nails	DeWalt 16 Gauge 1-1/4"	Table Saw	To trim cut MDF
Coating	West system - Epoxy Crown- Denatured Alcohol	DeWalt Air gun	Temporary hold until glue sets
Wood Dust	Wood dust from cutting of plywood	Air Compressor	Supply air for the experimental work
Glue	Epoxy	Drill Press	Drill holes for minor fittings

Figure 27 shows the Epoxy and Denatured Alcohol used for the experiment. The epoxy is a two part solution comprising of epoxy resin and epoxy hardener.

Figure 27. Epoxy resin, epoxy hardener and denatured alcohol

Figure 28 shows the MDF sheets, nail box and nail gun used for the experiment.

Figure 28. MDF sheet, nail and nail gun used in the experiment

Differential Pressure Transducer

Model 267 MR by SETRA was used to measure the internal and external pressure difference of the test box during the test. Figure 29 shows the SERTA model 267 MR

Figure 29. SETRA 267 MR differential pressure gauge

Table 3 shows the relationship between pressure, wind speeds and the readings given by the SETRA differential pressure transducer. The pressure gauge can measure the differential pressure between the inside and outside of the test box.

The outside volume is effectively infinite for this type of work and acts as a pressure sink. The inside volume represents the region of high pressure that will flow into the house. The key status is the time to pressure equalization due to the highly damped nature of the experimental set up.

Table 3.

Pressure and wind speed relationships

MODEL 267 MR Gauge Reading	Pressure kPa	Wind Velocity m/s	Wind Velocity mph	Pressure psf	Pressure psi
4.00	0.00	0.00	0.00	0.00	0.00
5.00	0.47	30.56	68.35	9.75	0.07
6.00	0.93	43.21	96.67	19.50	0.14
7.00	1.40	52.93	118.39	29.25	0.20
8.00	1.87	61.11	136.71	39.00	0.27
9.00	2.33	68.33	152.85	48.75	0.34
10.00	2.80	74.85	167.43	58.51	0.41
11.00	3.27	80.85	180.85	68.26	0.47
12.00	3.74	86.43	193.34	78.01	0.54
13.00	4.20	91.67	205.06	87.76	0.61
14.00	4.67	96.63	216.16	97.51	0.68
15.00	5.14	101.35	226.71	107.26	0.74
16.00	5.60	105.85	236.79	117.01	0.81
17.00	6.07	110.18	246.46	126.76	0.88
18.00	6.54	114.34	255.76	136.51	0.95

Data Collection Device

VersaLog DCVC- HR is a data logger used to log the entries acquired by the differential pressure transducer. The VersaLog requires a 120 volt power supply to operate and is connected to the computer using a USB cable. Site View software by ACCSENSE was used to record and graphically represent the data acquired by the VersaLog. Figure 30 shows the VersaLog DCVC – HR from the data sheet.

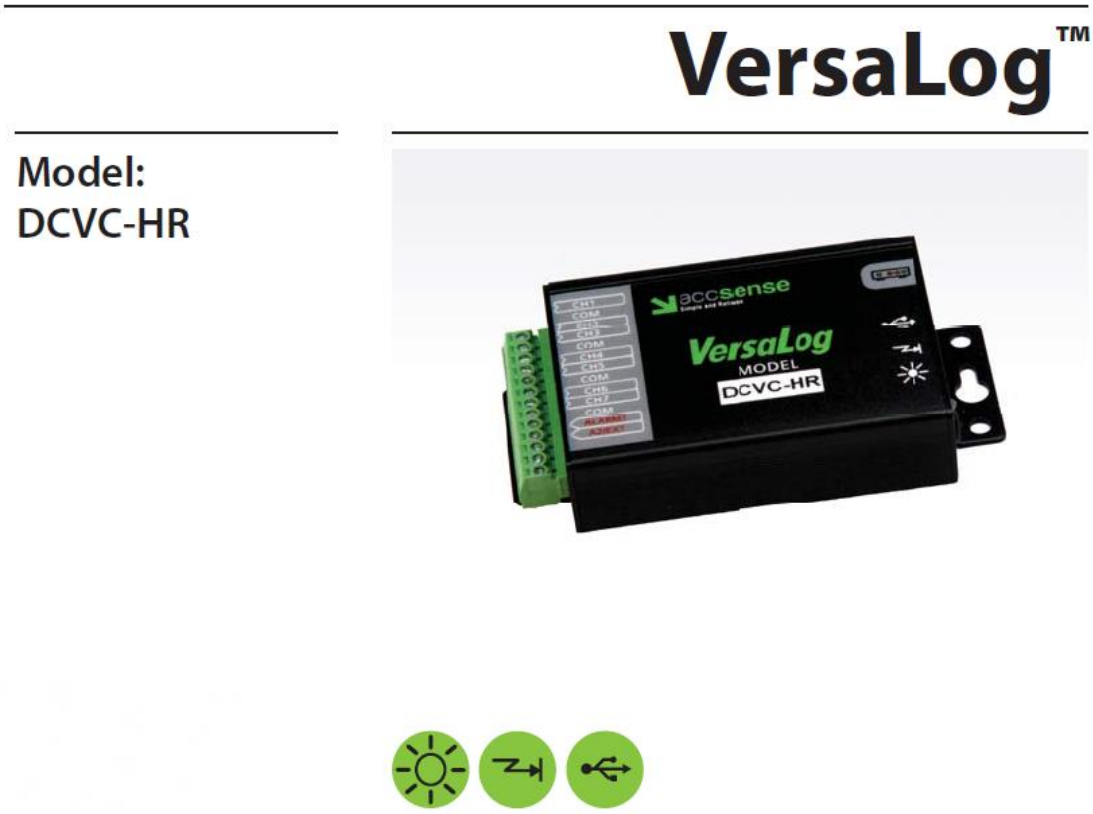

Figure 30. VersaLog DCVC – HR

Figure 31 and Figure 32 shows the data sheet provided by the manufacturer for VersaLog DCVC – HR.

Inputs

Channels	CH1 ~ CH4 (voltage): programmable range for each: 0 ~ 20 V, 0 ~ 2 V, CH5 ~ CH7 (current) programmable range for each: 0 ~ 20 mA
Accuracy	Thermistor channel: reference temperature 0.36°F
	Voltage channels: +/- 0.05% FSR @ 25°C for 20V channels, +/- 0.1% FSR @ 25°C for 2V channels
	Current channels: +/- 0.15% FSR @ 25°C
Load Resistor	For current channel: 12 Ohms
Protection	Voltage channel: +/- 40 VDC, Current channel: +/-100 mA

Alarms

Channel Alarms	Two editable alarm thresholds per channel
Alarm Outputs	ALARM1 & A2/EXT terminal strips can be configured as alarm outputs
	Alarm-On: MOSFET (N-Channel) switch on Alarm-Off: MOSFET (N-Channel) switch off
	Max Power: 200mA @ 24VDC
	Can report alarm status to host PC via USB, Modem or Ethernet Device Server with SiteView software[2]
Alarm-On Delay	Programmable 0 - 10 minutes delay with 1-minute increments
Alarm Indicator	On-board LED lights in red when in alarm condition

On-Board Memory

Capacity	4MB ~ 2 million measurements
Data Retention	Over 20 years

Sampling & Logging

Sampling Interval	20 milliseconds[1] to 12 hours user selectable
Logging Mode	Stop recording or FIFO when memory is full
Logging Activation	Programmable instant, start delay or field push-button activation

Figure 31. VersaLog DCVC – HR – Manufacturer's data sheet -1

Communications

Interface	USB (USB cable included), AUX (RJ11) for direct TTL level communications
	Can be connected to Ethernet for remote access with DeviceServer Kit[2]
Baud Rate	Auto-detect baud rate from 2400 to 115200 bps on both USB and AUX ports

Battery

Power	Built-in 3.6V Lithium Battery
Life Cycle	10 years based on 1 minute sampling interval

Software

SiteView[2]	Configuration, downloading, plotting, real-time view, custom calibration and custom equation
Software Requirements	Computer with 1.0 GHz or faster processor, 256 MB Memory or higher & 1.0 GB of available hard-drive space or higher
	Windows XP with SP2 or later, Vista, Windows 7, 8
	At least one USB port or one COM port

Other

LED Indicator	Normal Sampling: green when sampling Alarm: red when sampling Low Battery: amber when sampling
Excitation Control	A2/EXT terminal strip can be configured as excitation control output for powering connected devices
	Warm-up delay Interval settings: 10 to 240 seconds with 10-second increments
Operating Environment	-40 ~ +70°C (-40°F ~ 158°F), 0~95%RH non-condensing
Clock Accuracy	+/- 1 minute per month
Approvals	CE, FCC

[1]: Maximum enabled channel: 1 for 20ms interval, 2 for 30ms, 8 for 40ms or bigger interval.

[2]: Sold separately.

Figure 32. VersaLog DCVC – HR – Manufacturer's data sheet -2

Test Specimen

The plug whose friction failure is being tested in this research experiment is made of Ninja flex 3d printing filament (chemical name: Thermoplastic polyurethanes). The plug is circular in shape with a diameter of 30 mm. Two plugs, manufactured to the same nominal dimensions and from the same material are used in this experiment.

They are termed plug A and plug B respectively as seen in Figure 33.

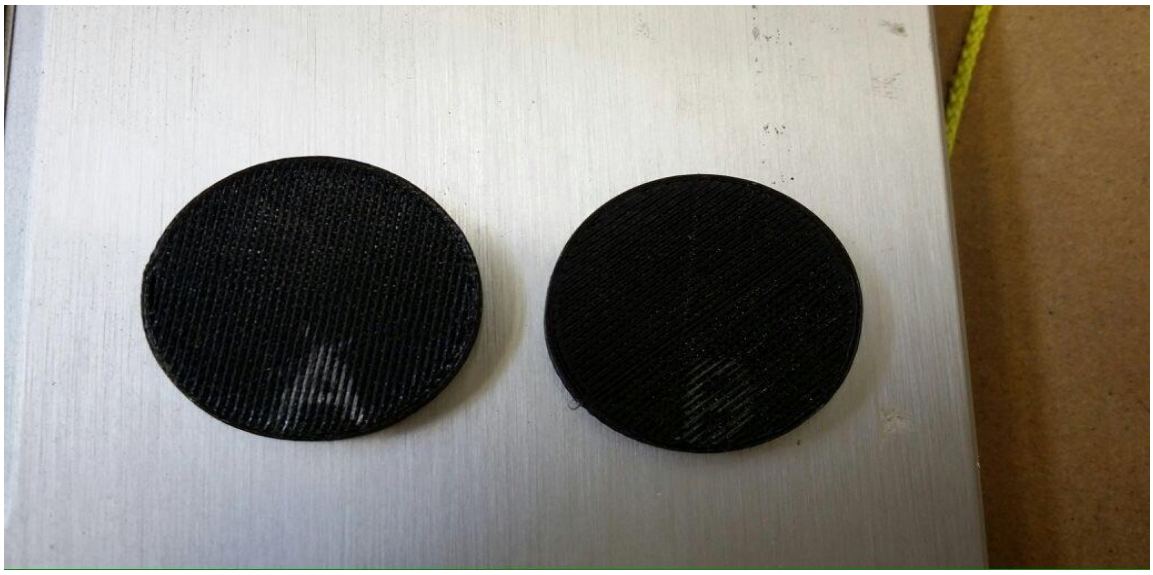

Figure 33. Plug A and Plug B

Construction of Test Apparatus

The box was equipped with the plug attached to a tube. The plug proves the weakest link in the assembly that will serve a pressure release opening to prevent the development of high wind forces causing damaging internal pressures. The plug is attached flush to the open end of the pipe extruding out of the test box. The purpose of

this experiment is to evaluate the consistency of the friction failure of the plug against wind loads.

Figure 34 shows the pipe extruding out of the test box and Figure 35 shows the plug attached flush to the assembly.

Figure 34. Pipe assembly attached to the test box

Figure 35. Plug attached to the pipe assembly

The test box was tested for pressure stability upon construction to map out any leaks in the assembly. The pressure was regulated through pressure gauge. Figure 36 shows the pressure gauge system.

Figure 36. Pressure gauge

Leak Sealing

Initial testing was accomplished by providing additional pressure without the use of any monitoring device. Several minor leaks were detected through the edges of the test box. The box was sealed by providing additional reinforcement to the top edges of the box. Additional strips of MDF were glued to the box with epoxy. All the joints and connections were reinforced by additional epoxy. Figure 37 shows the additional strips being held in place by clamps. Figure 38 shows the additional glue being applied to the edges.

Figure 37. Additional strips provided to the test box

Figure 38. Additional glue applied to the edges of test box

A safety valve was installed to prevent any accidents from occurring due to the development of high pressures inside the box. Figure 39 shows the safety valve installed in the test box.

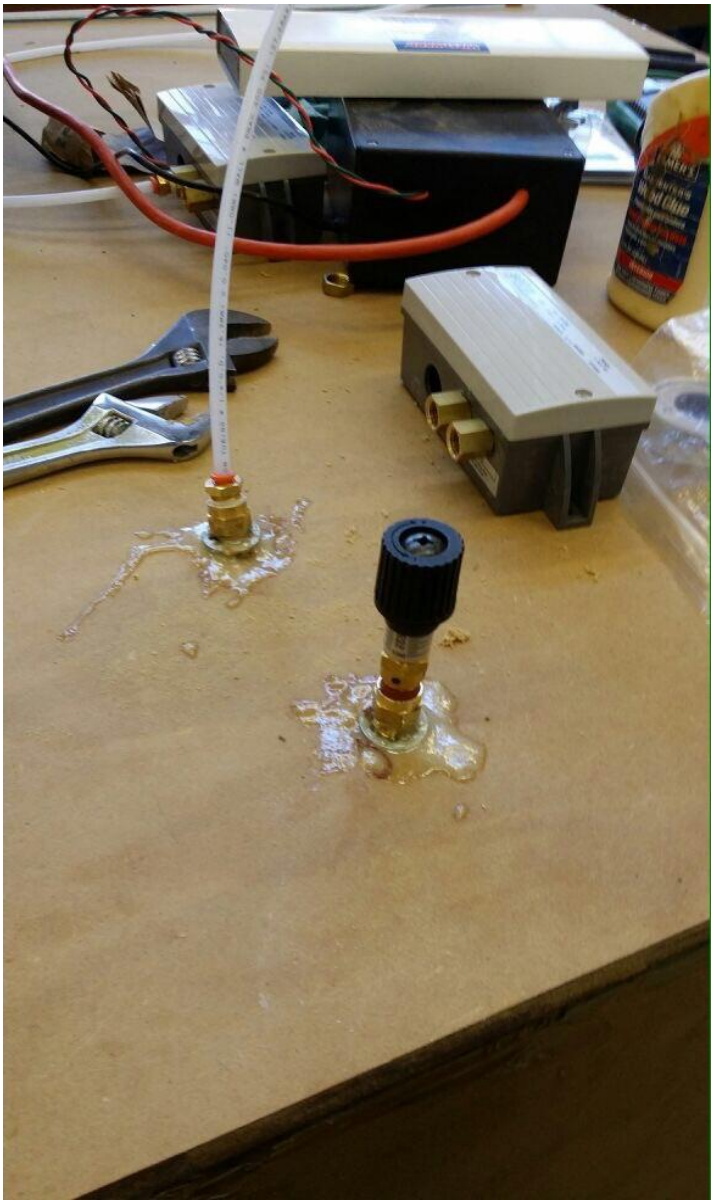

Figure 39. Safety valve

Test protocol

Test Series One – Pressure Testing of Stability of the Box

To conduct the pressure stability test, the current (mA) and Temperature (Degree Centigrade) were measured through a deferential pressure transducers. Site View ACCSENSE Versa Log was used to record the data. The steps were:

- The readings were taken for ten minutes with a reading interval of 100 millisecond at 0 psi additional pressure and recorded.
- Another set of readings were taken for ten minutes with a reading interval of 100 millisecond at 30 psi
- The readings at 30 psi were repeated two more times for consistency
- All the data collected from the above mentioned readings were entered in Microsoft EXCEL to analyze and compare results

Subsequent Test Series

Two sample plugs, plug A and plug B were manufactured at TAMU architecture using a 3D printing machine. To conduct the test the steps were:

- the pressure was increased gradually through pressure valves to the point when the plug ejects from the shaft
- The current (mA) and Temperature (Degree Centigrade) were measured through a deferential pressure transducer
- Site View ACCSENSE Versa Log was used to record the data

- The experiment was repeated 100 times for both Plug A and Plug B for consistency. All the data collected from the above mentioned readings were entered in Microsoft EXCEL to analyze and compare results

Summary

The experimental work is designed to apply a pressure to the inside of a timber box until the pressure plug fails. The equipment records the differential pressure with time for the experiment.

CHAPTER IV

RESULTS

Introduction

This chapter outlines the results for the experimental work. Three series of test are conducted in this experiment. The first test series was performed to check the stability of the test box under applied pressure. In the first test series, three sets of readings are taken, one set at zero additional pressure and two sets at 30 psi additional pressure. The second and third test series are performed to check the friction factor of two identical plugs, plug A and plug B.

Test series one

Test Series One: Part One

Part One of Test Series One tests the testing box at zero additional pressure. The readings are taken for a total of 10 minutes. 6000 readings are taken at the interval of 100 millisecond. Table 4 summarizes the test basic data.

Table 4.

Test one part one details

Description	Unit
Test Date	18 February 2015
Number of Readings	6000

The readings form the part one of test series one logged on to EXCEL. Summary statistics is calculated as shown in Table 5.

Table 5.

Summary statistics for test series one: part one

Description	Number
Mean	4.014855857
Standard Error	0.000130575
Median	4.01
Mode	4.01
Standard Deviation	0.010115173
Sample Variance	0.000102317
Kurtosis	-.079360238
Skewness	0.024785693
Range	0.07
Minimum	3.98
Maximum	4.05
Sum	24093.15
Count	6001
Largest(1)	4.05
Smallest(1)	3.98
Confidence Level (95.0%)	0.000255975

This tests series was designed to ensure that the system operated as designed and that consistent results were obtained from the experimental equipment.

Test Series One: Part Two

Part Two of the Test Series One tests the testing box at an inlet additional pressure of 30 psi applied through the high pressure air system. A total of 6000 readings are taken at the interval of 100 millisecond. The pressure in the box is measured to check for experimental consistency. Table 6 shows the test details.

Table 6.

Test one part two details

Description	Unit
Test Date	18 February 2015
Number of Readings	6000

The readings are logged in MS Excel. The summary statistics are calculated for the recorded readings as shown in Table 7.

Table 7.

Summary statistics for test series one: part two

Description	Number
Mean	9.733011165
Standard Error	0.000666263
Median	9.73
Mode	9.7
Standard Deviation	0.051612802
Sample Variance	0.002663881
Kurtosis	-.481984958
Skewness	0.439265852
Range	0.26
Minimum	9.62
Maximum	9.88
Sum	58407.8
Count	6001
Largest(1)	9.88
Smallest(1)	9.62
Confidence Level (95.0%)	0.001306115

The results are consistent.

Test Series One: Part Three

Part Three of Test Series One is performed to check the consistency of results acquired from part two of test series one. A total of 6000 readings are taken at 30 psi external pressure. The reading interval is of 100 milliseconds.

Table 8.

Test one part three details

Description	Unit
Test Date	18 February 2015
Number of Readings	6000

The readings are logged in MS Excel. The summary statistics are calculated for the recorded readings as shown in Table 9.

Table 9.

Summary statistics for test series one: part three

Description	Number
Mean	9.926878854
Standard Error	0.000451498
Median	9.93
Mode	9.95
Standard Deviation	0.034975803
Sample Variance	0.001223307
Kurtosis	-.954965921
Skewness	-0.06463119
Range	0.17
Minimum	9.84
Maximum	10.01
Sum	59571.2
Count	6001
Largest(1)	10.01
Smallest(1)	9.84
Confidence Level (95.0%)	0.000885098

The results are consistent.

Summary

The results show that the test box gives consistent readings for the entire test period of 10 minutes, the variation in the readings are statistically insignificant at zero additional pressure. The test results for part one and two are very constant and the variation in the readings are statistically insignificant for both sets of readings. Based on the summary statistics, it can be concluded that the box is stable under additional pressure and will hold a desired level of pressure without any outflows within an acceptable range of tolerance.

Test series two

Test Results

The second test series investigates the response of Plug A to applied wind pressure. Test series two consists of 100 readings for Plug A as shown in Table 10.

Table 10.

Test two details

Description	Unit
Test Date	27 February 2015
Number of Readings	100

The readings taken by the differential pressure transducer are taken in form of milliamps. These readings are then converted from milliamps to pounds per square foot. The conversion graph is shown in Figure 40.

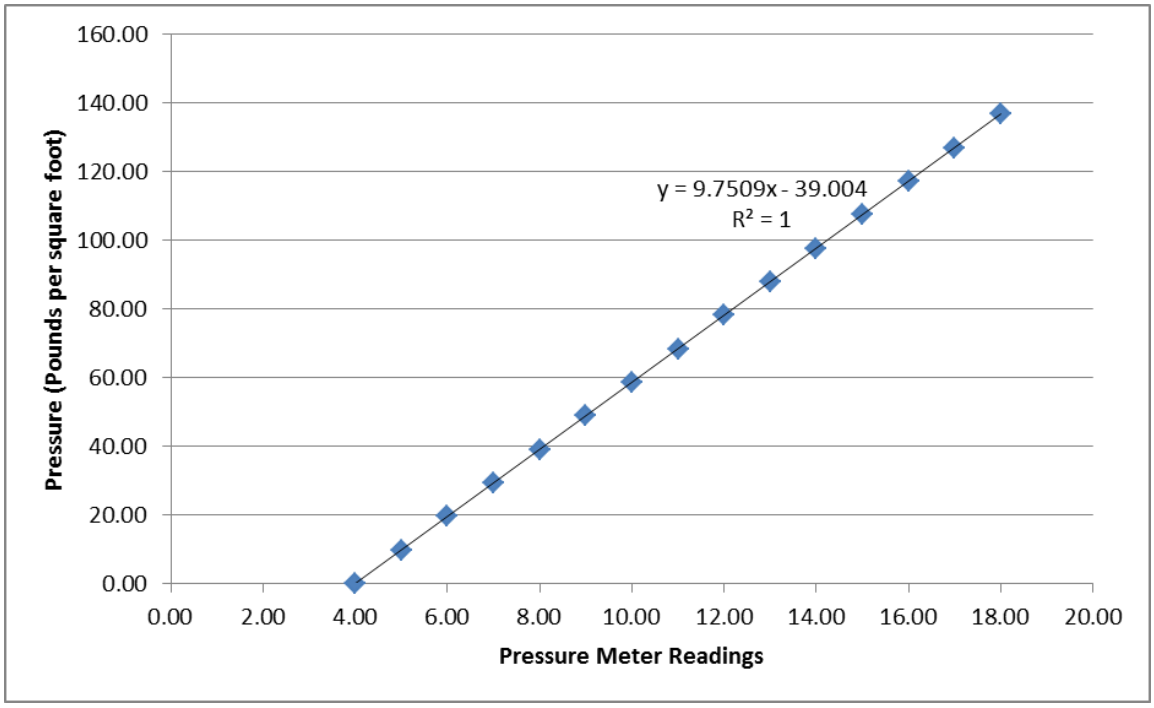

Figure 40. Conversion of pressure meter readings to pressure in pounds per square foot

Figure 41 shows one the readings from the test series two as seen in the Site view computer program.

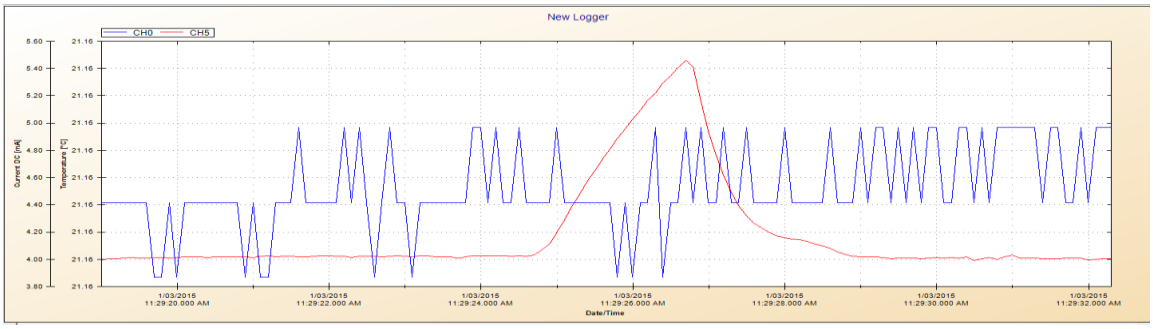

Figure 41. A reading from test series two as seen in Siteview computer software

Figure 41 presents the critical result for the experimental work. The blue line on the graph shows the temperature during the test period. The steps reflect the digital nature of the data. The red line shows the pressure readings. The start of the test can be seen in the readings followed by a gradual increase in pressure up to the point of failure of the plug. The heavily damped response can be seen in the outflow. A rapid drop off would suggest that a resonator was feasible and require a modification of the experimental procedure. The readings from test series two are tabulated in Table 11 and Table 12.

Table 11.

Readings from test series two – set 1

Number	Test	N	Test	N	Test	N	Test	N	Test
1	14.23591	11	18.03877	21	16.38111	31	19.5014	41	16.86866
2	14.91848	12	16.77115	22	15.30851	32	16.47862	42	16.18609
3	16.96617	13	15.40602	23	16.18609	33	15.79606	43	13.55335
4	16.57613	14	15.89357	24	15.30851	34	16.38111	44	14.33342
5	16.38111	15	15.89357	25	17.25869	35	15.30851	45	16.86866
6	15.50353	16	16.96617	26	19.98895	36	15.99108	46	15.50353
7	18.23378	17	15.50353	27	15.01599	37	15.99108	47	16.08859
8	16.86866	18	15.01599	28	19.59891	38	15.69855	48	13.74837
9	16.96617	19	15.50353	29	14.72346	39	14.23591	49	14.13841
10	15.40602	20	15.79606	30	16.08859	40	15.60104	50	15.30851

Table 12.

Readings from test series two – set 2

Number	Test	N	Test	N	Test	N	Test	N	Test
51	13.74837	61	15.99108	71	16.18609	81	17.45371	91	18.72133
52	16.57613	62	18.13627	72	13.74837	82	15.211	92	14.0409
53	14.52844	63	14.82097	73	15.60104	83	16.96617	93	16.2836
54	17.74624	64	14.13841	74	12.77328	84	15.99108	94	15.30851
55	14.72346	65	16.77115	75	13.45584	85	15.01599	95	14.82097
56	13.94339	66	19.40389	76	14.33342	86	16.67364	96	18.23378
57	14.72346	67	15.1135	77	15.01599	87	12.77328	97	14.52844
58	15.40602	68	12.67577	78	15.79606	88	13.45584	98	15.50353
59	17.45371	69	14.23591	79	23.69429	89	18.52631	99	13.84588
60	15.40602	70	15.50353	80	18.23378	90	19.20887	100	15.89357

Table 13 shows the summary statistics for the readings.

Table 13

Summary statistics for test series two readings

Description	Value	Unit
Mean Value – all tests	14.355	lb/ft^3
Standard deviation – all tests	1.762	lb/ft^3
Median – all tests	15.601	lb/ft^3

Figure 42 & Figure 43 shows the graphical representation of the pounds per square foot conversion for the readings.

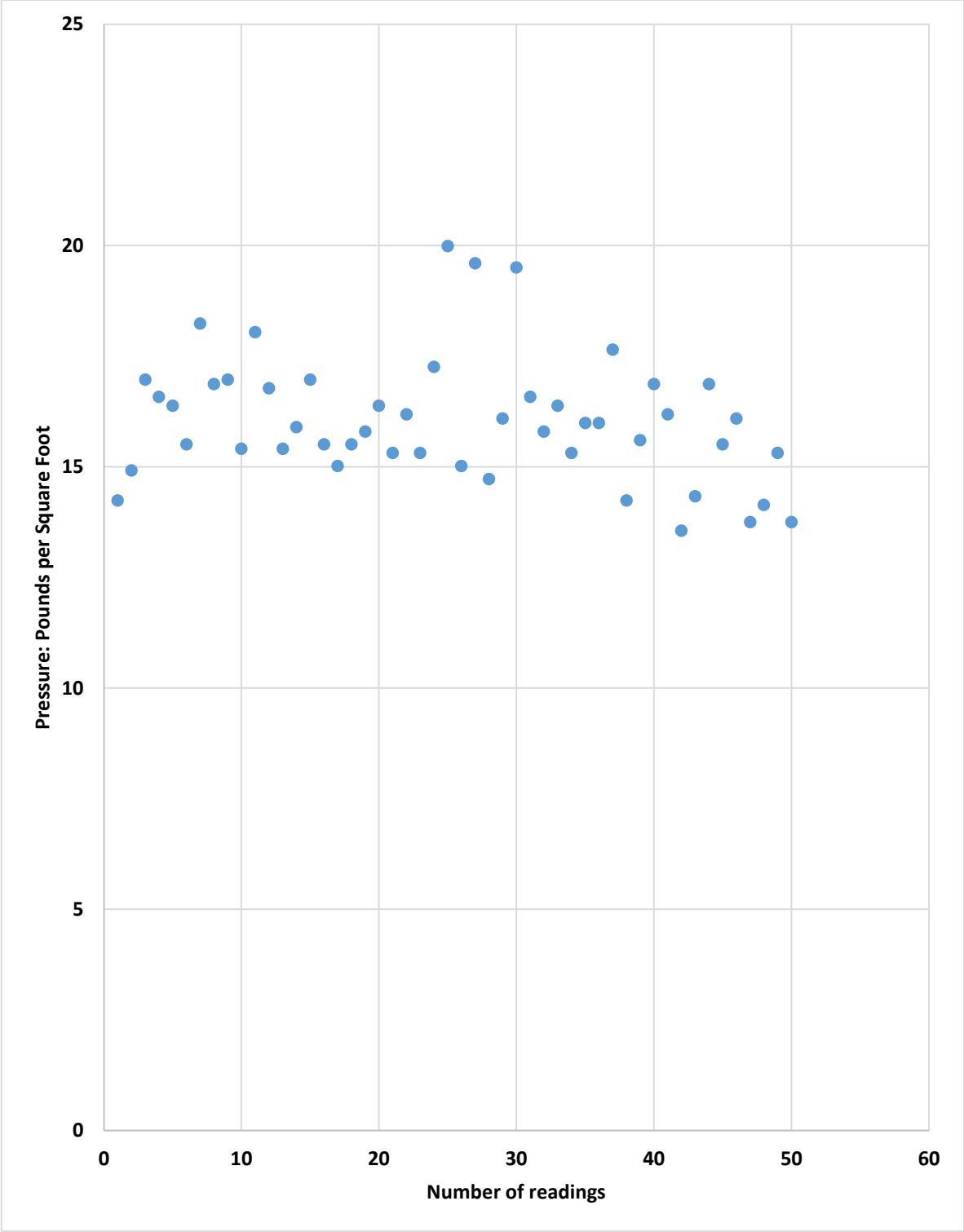

Figure 42. Data plot of readings 1-50 from test series two

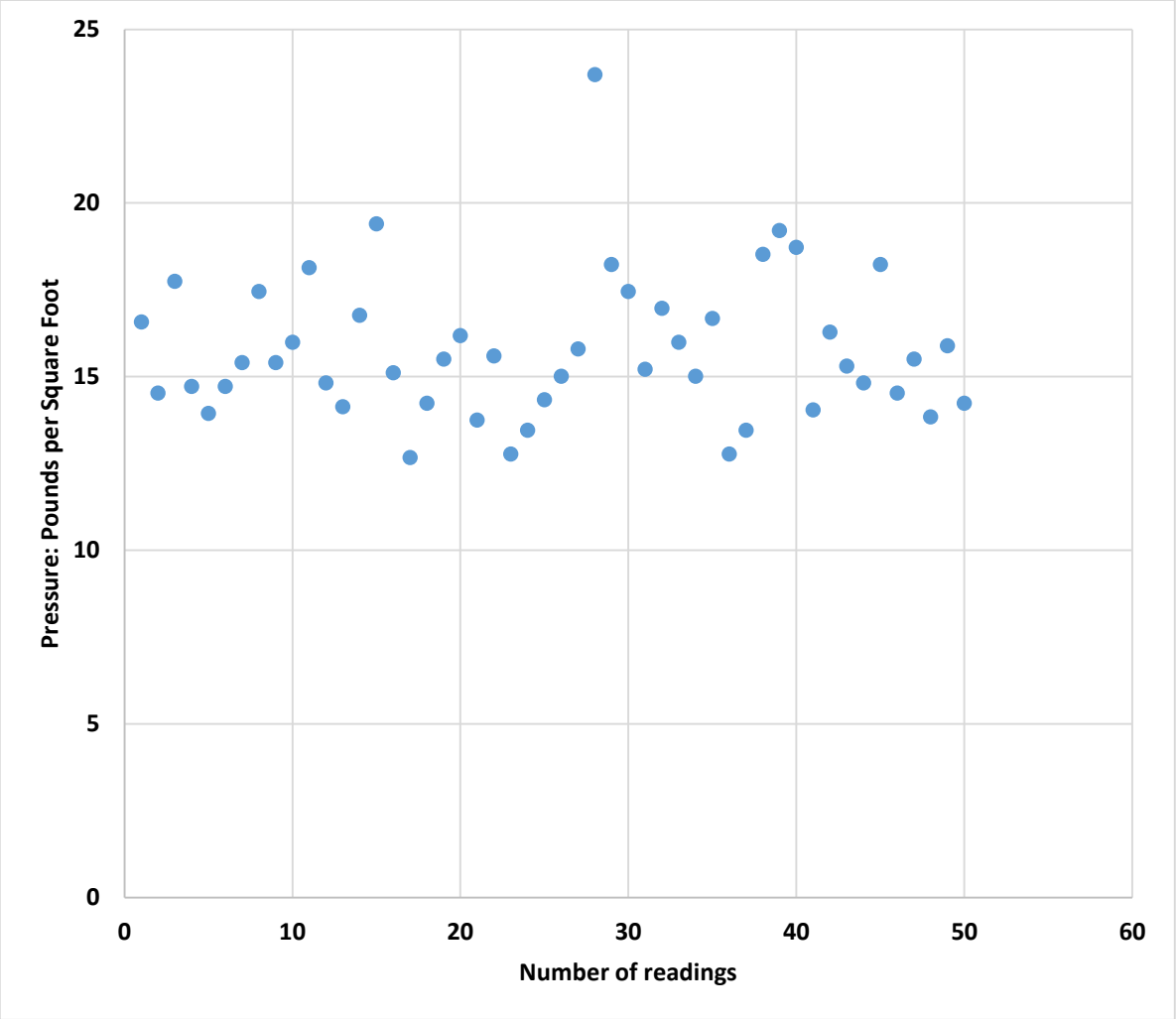

Figure 43. Data plot of readings 51-100 from test series two

Figure 44 shows the residual variable plot and the line fit plot from linear regression analysis.

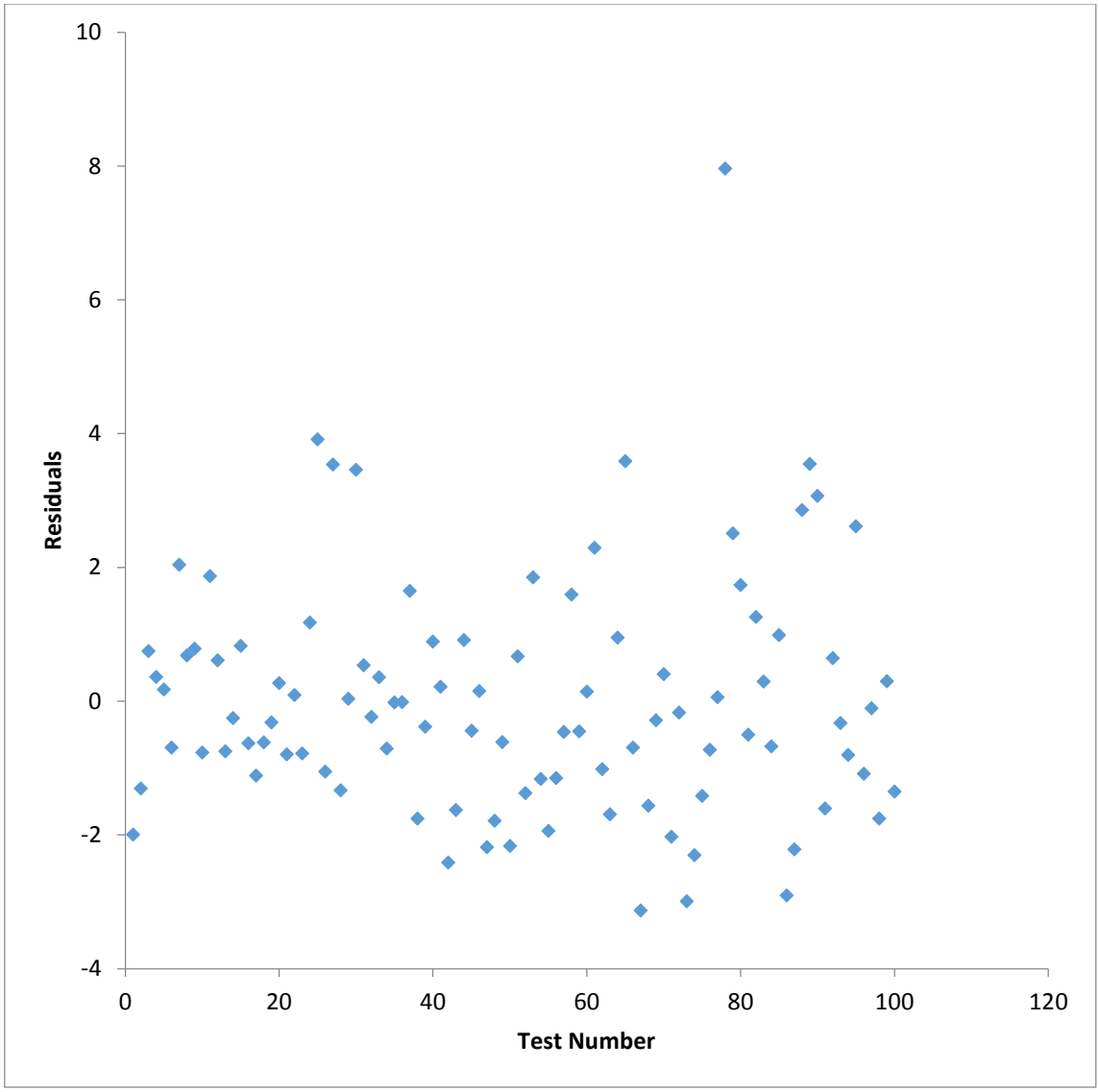

Figure 44. Residual value plot and the fit line plot for the test series two readings

Normality of the Data

The normal probability plot as seen in Figure 45 shows that the entire data set is Gaussian. The data set looks normally distributed apart form one outlier.

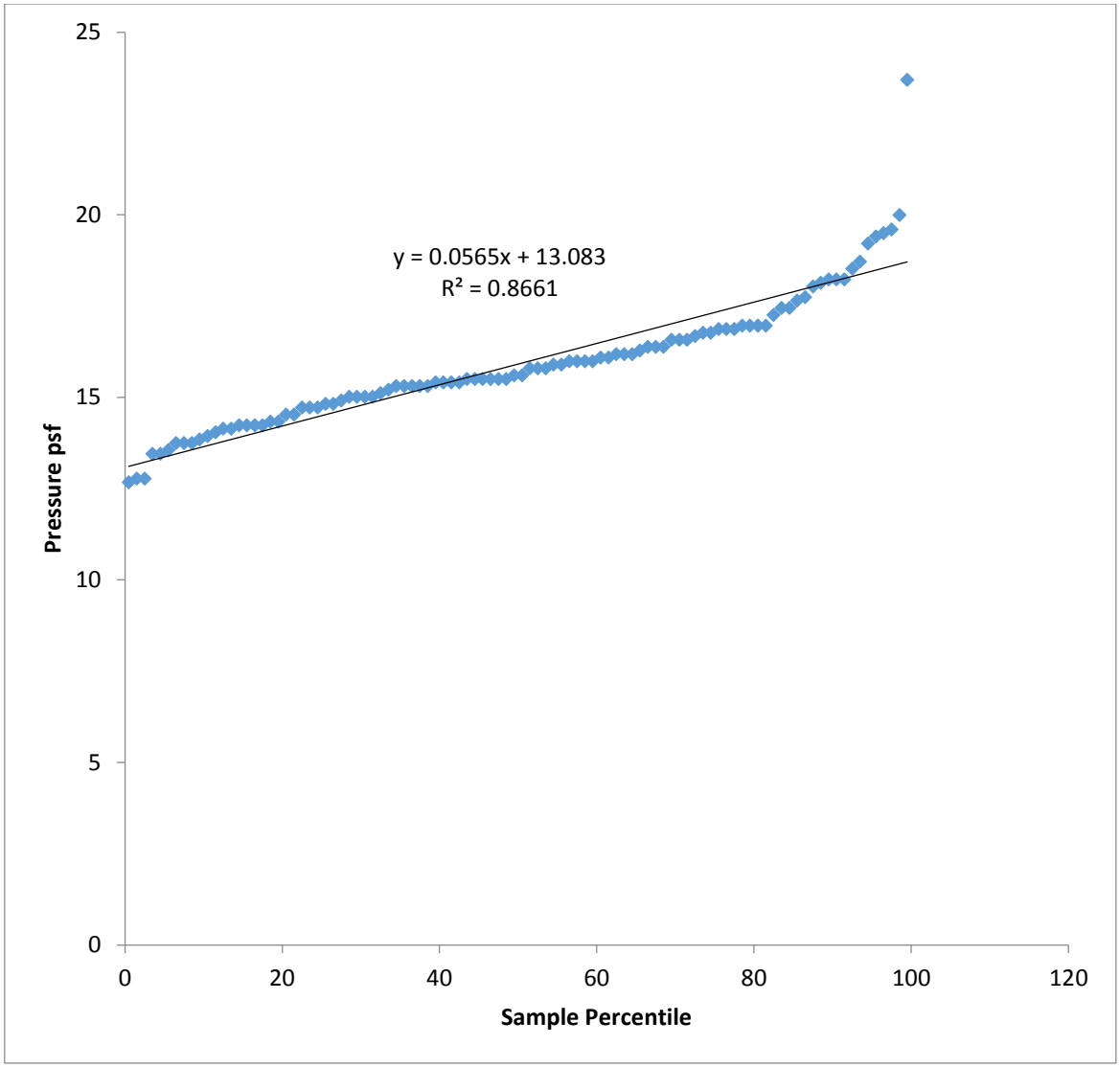

Figure 45. Normal probability plot for the test series two readings

T test: two samples assuming unequal variance

The readings are divided into sets of fifty readings each and a T test two samples assuming unequal variances is performed in Excel. The results for the T test are shown in Table 14.

Table 14.

Students t-Test results for test series two readings

Description	Variable 1	Variable 2
Mean	16.04373086	15.7765562
Variance	2.010345429	4.230480138
Observations	50	50
Hypothesized Mean Difference	0	
df	87	
t Stat	0.756239305	
P(T<=t) one-tail	0.225774318	
t Critical one-tail	1.662557349	
P(T<=t) two-tail	0.451548636	
t Critical two-tail	1.987608282	

Summary

The change in the means of the two data set is not statistically significant. Based on the regression analysis the data also seems to be normally distributed. On the basis of the above statistical analysis, it can be observed that the plug will function as required within an acceptable tolerance range.

Test series three

Test Results

Test series two consists of 100 readings for Plug B. Table 15 shows the test details for the second series with Plug B.

Table 15

Test Details

Description	Unit
Test Date	03 March 2015
Number of Readings	100

The same procedure as test series two for converting the values from milliamps to pounds per square foot is used.

Figure 486 shows one of the readings from the data set as seen in SiteView computer programme.

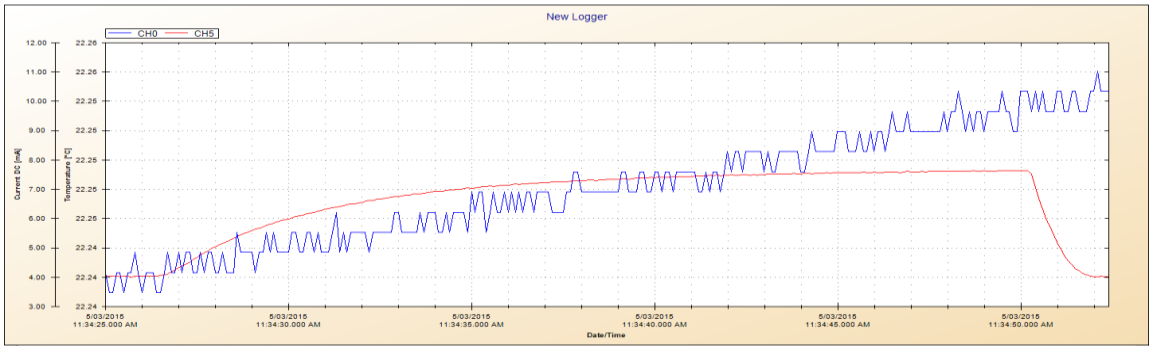

Figure 46. A reading from test series three as seen in Siteview computer software

The readings for test three are tabulated in Table 16 and Table 17.

Table 16.

Readings for test three - 1

Number	Test	N	Test	N	Test	N	Test	N	Test
1	43.48861	11	39.29573	21	33.64021	31	29.73985	41	41.92847
2	40.75836	12	44.07367	22	30.03237	32	35.39537	42	31.78753
3	35.39537	13	40.0758	23	30.22739	33	33.15266	43	30.22739
4	35.00533	14	32.37259	24	28.27721	34	30.22739	44	35.98042
5	30.51992	15	31.69003	25	27.49714	35	42.221	45	38.71067
6	31.20248	16	33.83522	26	30.71494	36	29.34981	46	34.03024
7	37.15053	17	39.19822	27	41.92847	37	31.29999	47	29.83735
8	40.56334	18	41.44093	28	32.37259	38	36.07793	48	39.88078
9	33.64021	19	29.73985	29	30.22739	39	39.19822	49	39.19822
10	32.95764	20	31.3975	30	29.15479	40	25.64447	50	25.93699

Table 17.

Readings for test three - 2

N	Test	N	Test	N	Test	N	Test	N	Test
51	35.20035	61	30.71494	71	26.42454	81	41.44093	91	35.00533
52	42.12349	62	33.25017	72	35.10284	82	30.3249	92	34.22526
53	30.90995	63	32.95764	73	44.85374	83	32.76262	93	25.35194
54	35.7854	64	30.90995	74	42.41602	84	42.90356	94	30.81244
55	38.61316	65	31.78753	75	23.49927	85	26.22952	95	35.00533
56	35.98042	66	31.10497	76	23.59678	86	26.52205	96	30.51992
57	35.7854	67	24.9619	77	41.53843	87	27.49714	97	43.00107
58	32.56761	68	35.29786	78	35.49288	88	31.3975	98	39.58825
59	39.97829	69	32.56761	79	44.75623	89	30.71494	99	29.44732
60	24.76689	70	33.15266	80	34.6153	90	35.29786	100	35.20035

Table 18 shows the summary statistics for the readings.

Table 18.

Summary statistics for test series three readings

Description	Value	Unit
Mean Value – all tests	34.016	lb/ft^3
Standard deviation – all tests	33.201	lb/ft^3
Median – all tests	15.601	lb/ft^3

Figure 487 and Figure 48 shows the graphical representation of the pounds per square foot conversion for the readings.

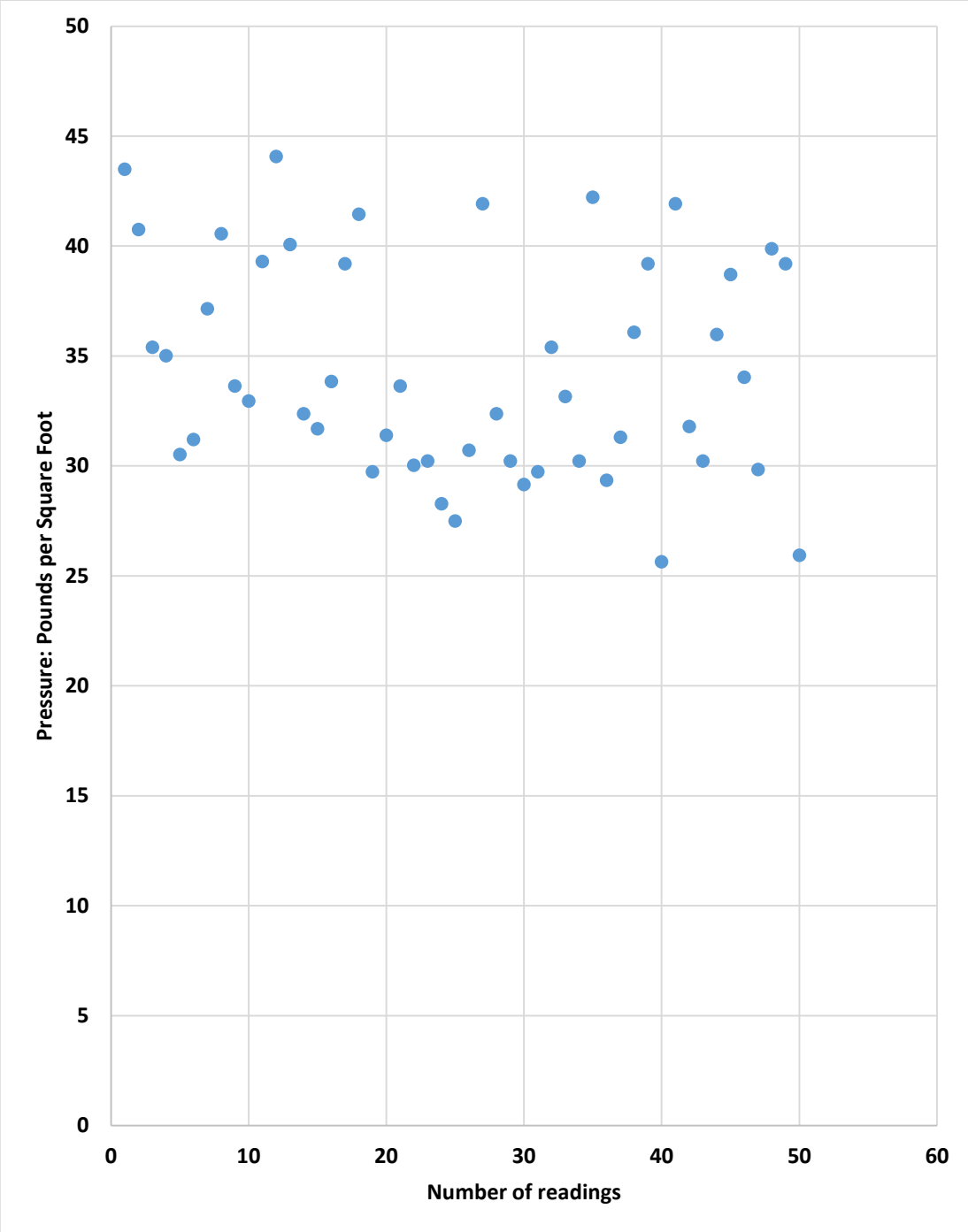

Figure 47. Data plot of readings from test series three readings - 1

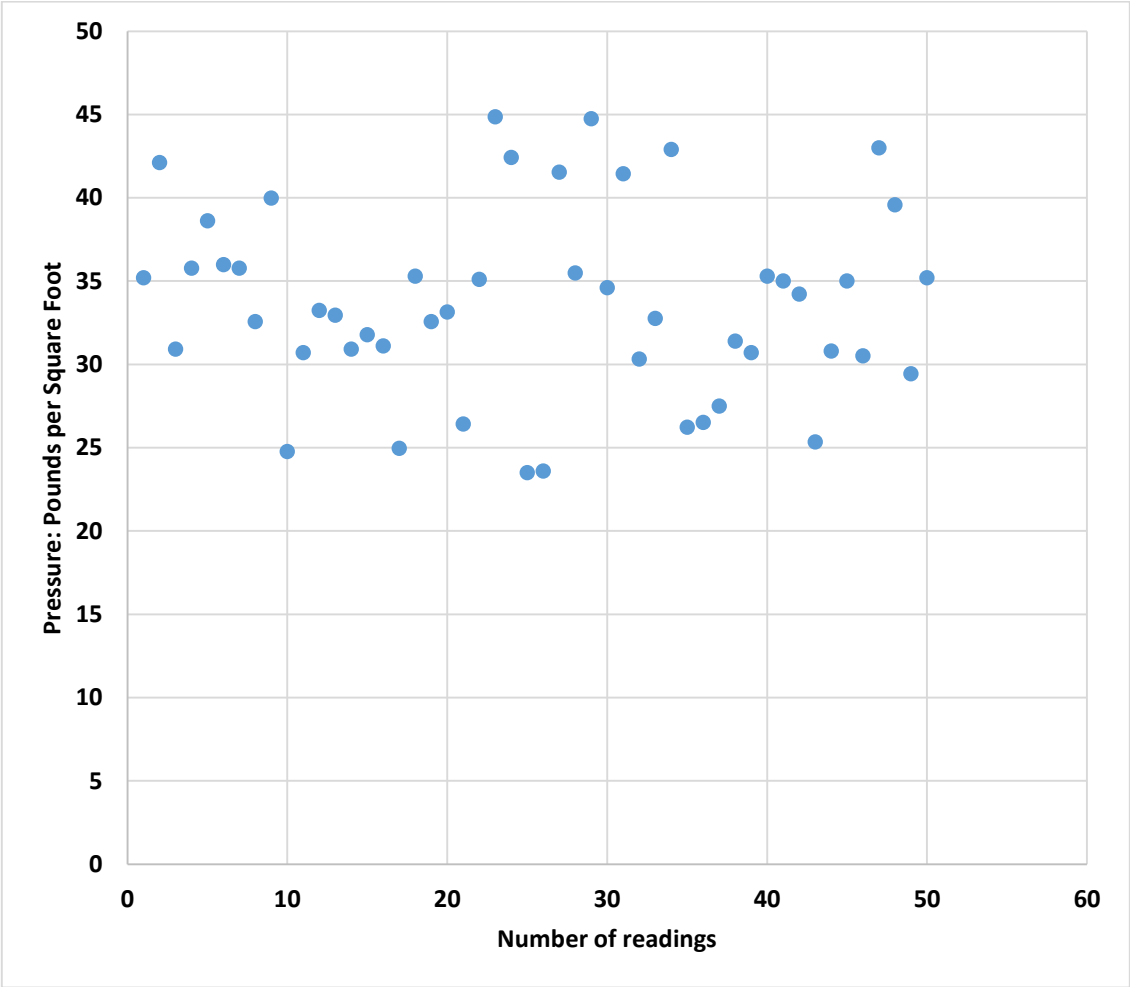

Figure 48. Data plot of readings from test series three readings - 2

Figure 49 shows the residual variable plot from linear regression analysis.

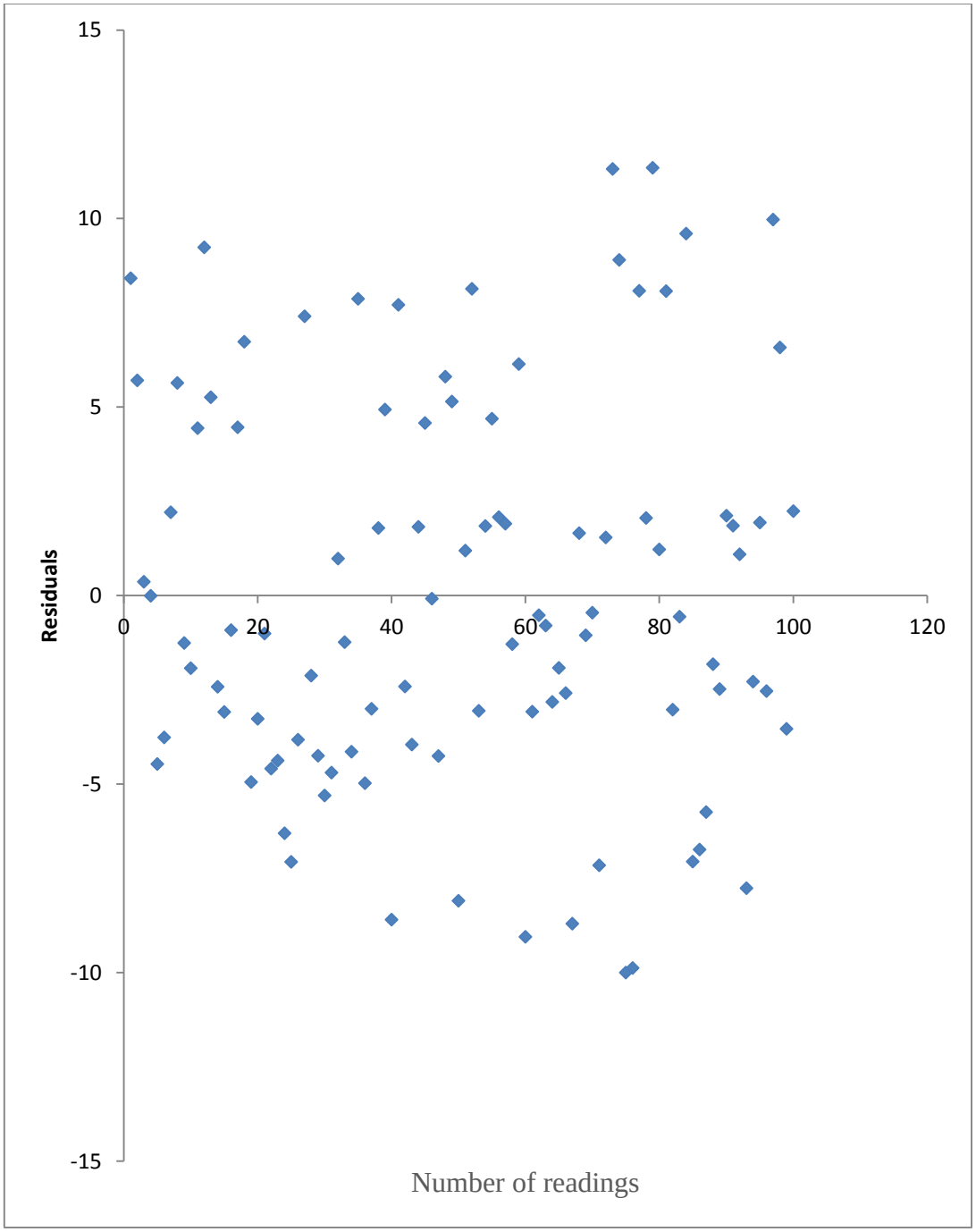

Figure 49. Variable residual plot for test series three readings

Figure 50 shows the line fit plot from the regression analysis.

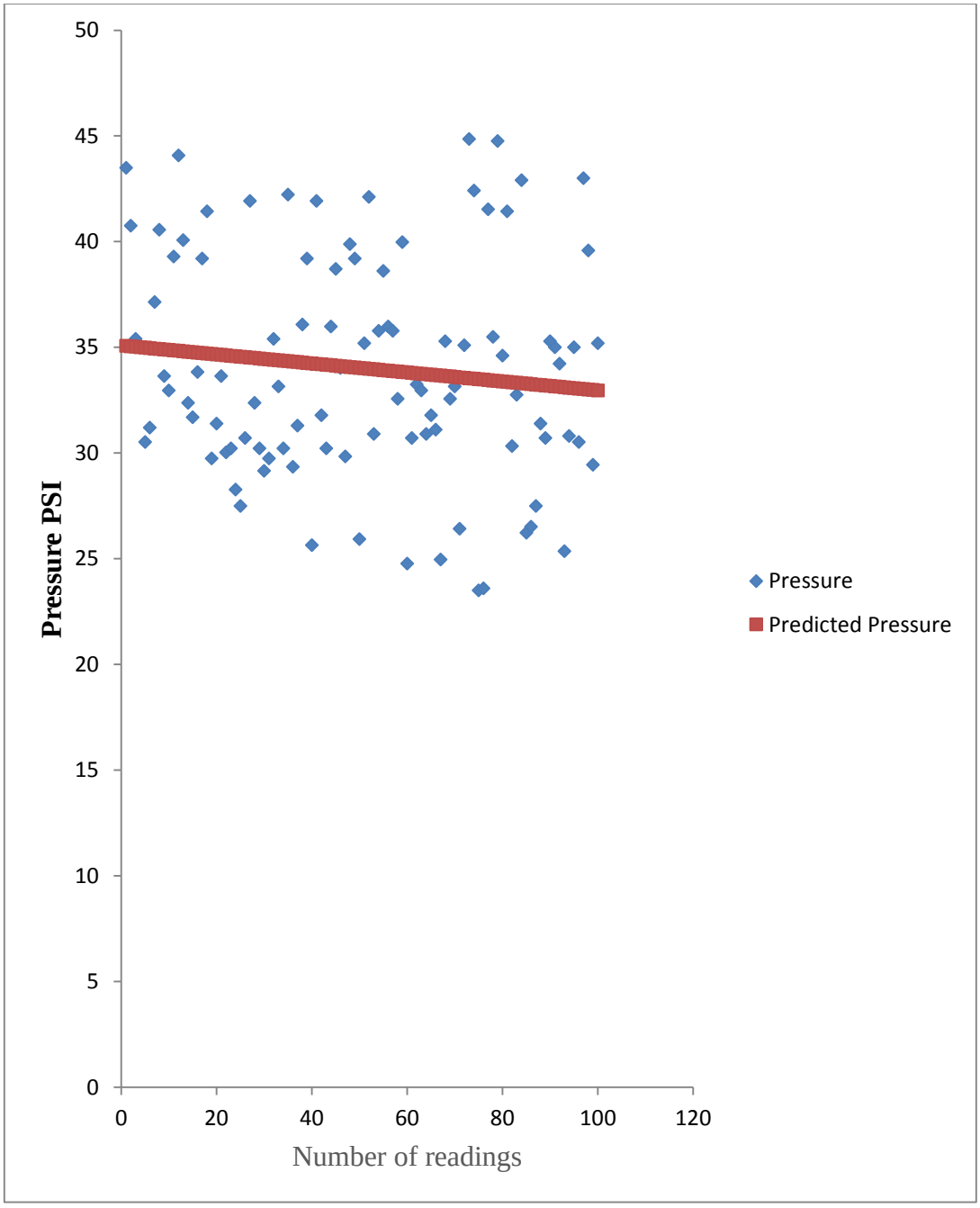

Figure 50. Fit line plot for test series three readings

The line fit plot appears to be scattered and inconsistent with the mean value.

Normality of the Data

The normal probability plot is shown in Figure 51.

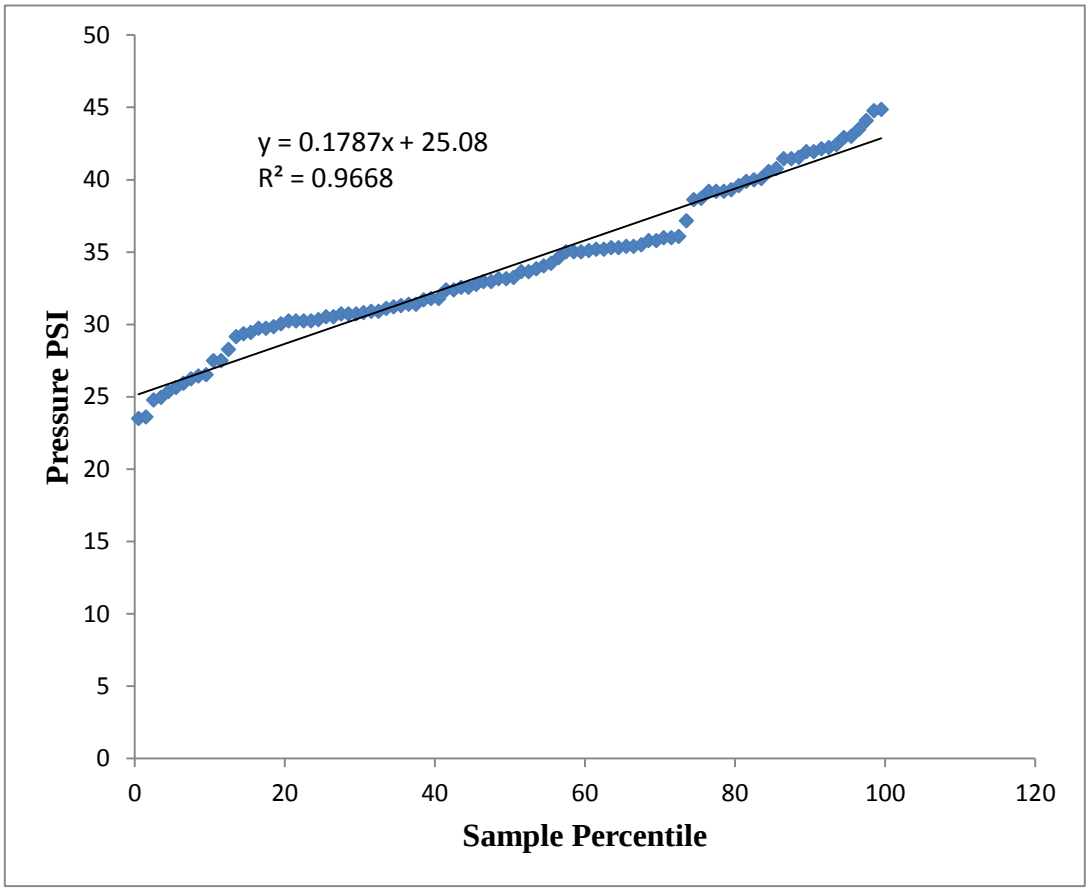

Figure 51. Normal probability plot for the test series three data

T test: Two samples assuming unequal variance

The readings are divided into sets of fifty readings each and a T test two samples assuming unequal variances is performed in Excel. The results for the T test are shown in Table 19.

Table 19

Students t-Test results for test series three readings

Description	Variable 1	Variable 2
Mean	34.35397	33.67921
Variance	24.33096	31.62828
Observations	50	50
Hypothesized Mean Difference	0	
df	96	
t Stat	0.637823	
P(T<=t) one-tail	0.262554	
t Critical one-tail	1.660881	
P(T<=t) two-tail	0.525108	
t Critical two-tail	1.984984	

Summary

Owing to the large variance found in the statistical analysis, and the inconstancy seen in the scatter plot. The plug B cannot be assumed to work consistently in an acceptable tolerance range.

Microscopic analysis of the plugs

Plug A performed with accuracy, whilst Plug B showed significant scatter in the results. A microscopic analysis of the two plugs was completed to determine if a difference exists in the manufacture of the plugs. The point of the tests is to provide repeatability in the results, with accuracy and precision.

Microscopic images of plug A and plug B can be seen in Figure 52 and Figure 53. Plug A is on the left in the photographs.

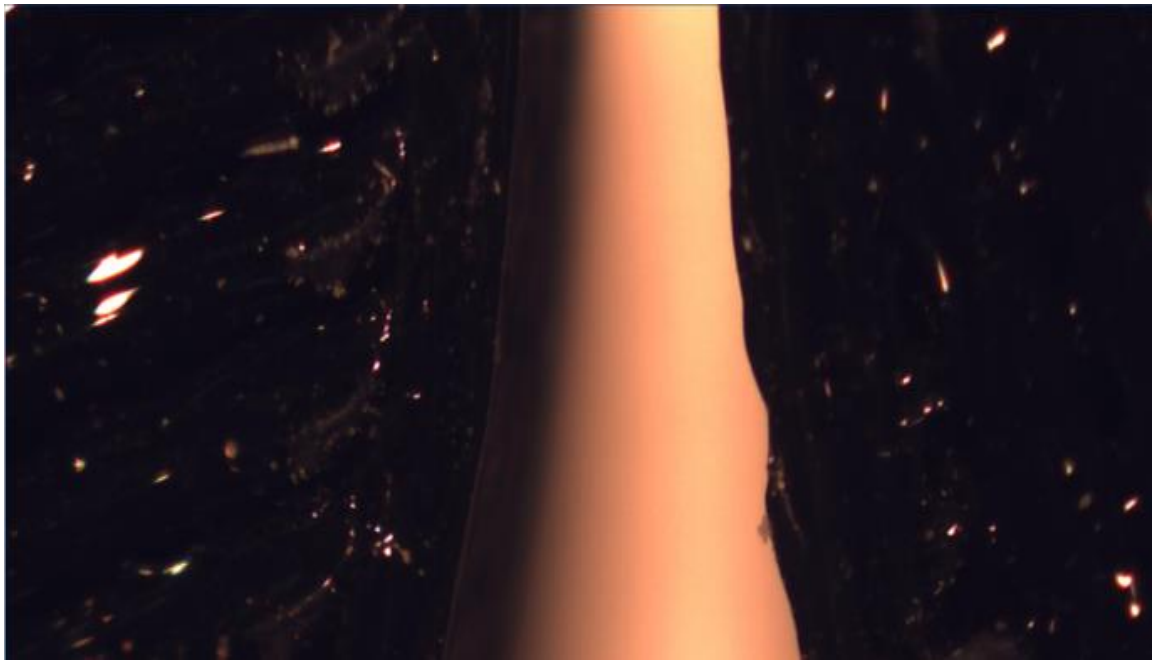

Figure 52. Microscopic images of plug A and plug B

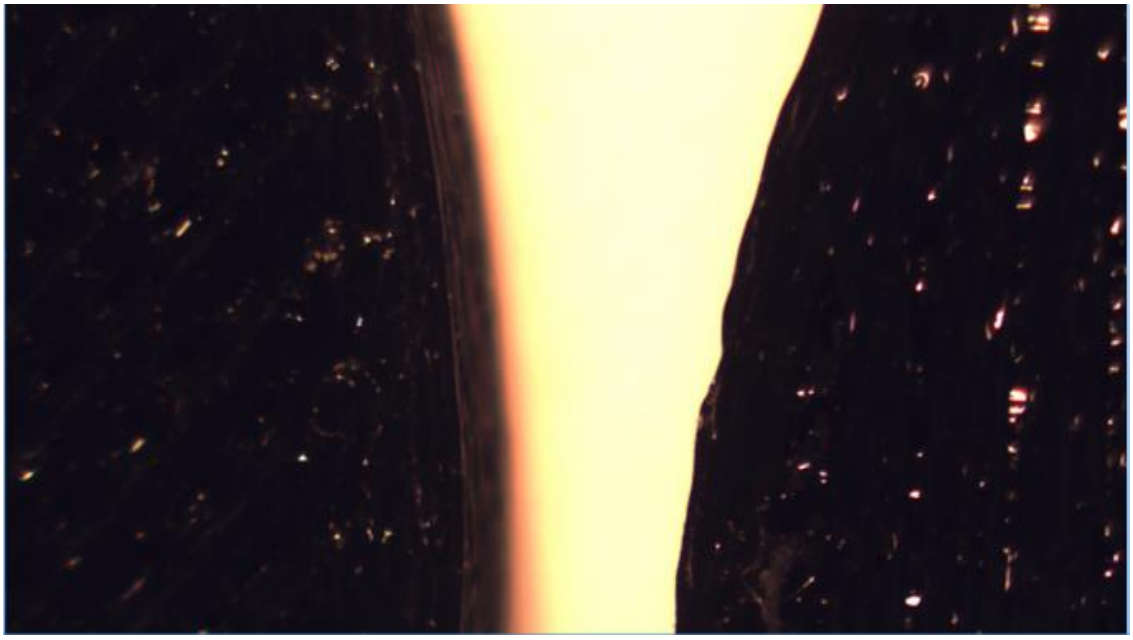

Figure 53. Microscopic images of plug A and plug B

Figure 54 and Figure 55 show the enlarged microscopic images of plug A and plug B respectively.

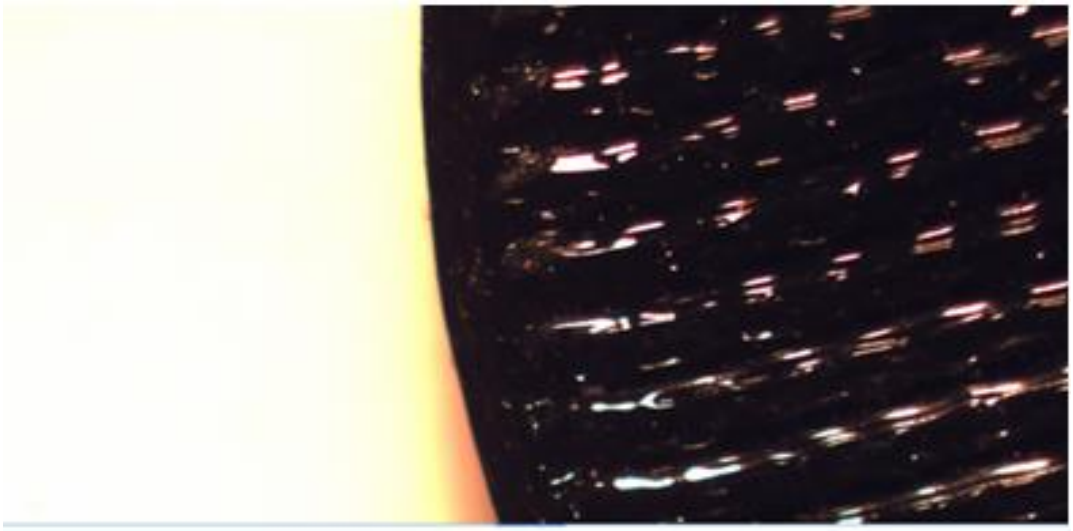

Figure 54. Microscopic image of plug A

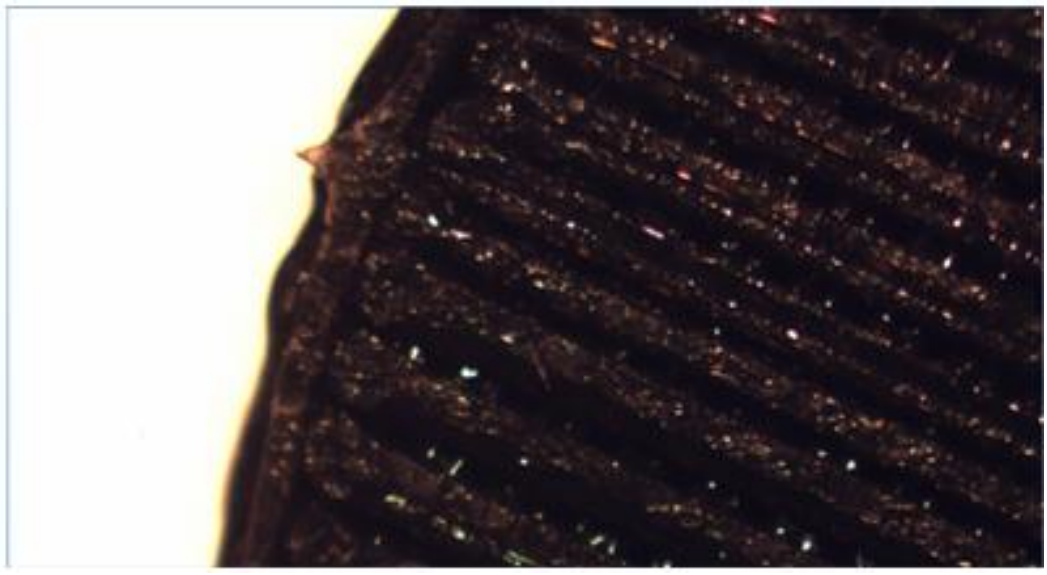

Figure 55. Microscopic image of plug B

Clearly Plug B is rougher on the friction edge than Plug A. This observation is considered to explain the difference in the pressure result accuracy between the two sets of data.

CHAPTER V

CONCLUSIONS

The ability of a house or small commercial building to withstand wind loads is often dependent on factors outside the control of the designer and builder. One of the common methods for house failure in a cyclonic event is a failure of a window during the event. Flying debris common in major wind events and windows are susceptible to damage.

A significant body of research commencing with work after Cyclone Tracy in 1974 has shown the cause of the roof loss is often the Helmholtz resonance induced when a window fails. Helmholtz resonance like all resonance is heavily dependent on the level of damping built into the system. The failure of a large plate glass window in a small room is not going to provide a sufficient level of damping to impact the slug of air accelerated into the building by the high pressure static zone on the windward side of the building.

American Society of Civil Engineers and Structural Engineering Institute (2010) provides a guide as to an acceptable, to the engineering community, window size for sufficient damping to occur in the. A simple characteristic length measure has been developed based on this idea. The length defined as λ provides a measure of the available damping. λ for a typical small room for the American Society of Civil Engineers and Structural Engineering Institute (2010) small window size will be in the order of 350.

This experimental work investigates the development of a test box that can model a high pressure wind storm and its impact on a plug set to model a failing window. The

test arrangement for this work used a 30 mm diameter plug, and a box size of one cubic meter, which results in a λ of 35.

Two experimental plugs were manufactured using NinjaFlex as the material. A simple pipe system was added to the test box to test the plugs. Each plug has a friction fit in the pipe.

Two observations can be seen in the results. The first is that the plug manufacture is not consistent. The plugs are not a good mechanism to model a failing glass panel. The second observation is that the box system worked well in terms of the accuracy of measurement when the plug was well formed.

The experimental hypothesis was that the failure of the pressure plug will equalize internal and external pressures for the box in a highly damped manner.

Based upon the results of the experiments described here, the hypothesis is confirmed. The system works and provides a system able to investigate failures of elements in a house. It is significantly simpler to use than a wind tunnel. It is recommended that the system be developed to create a low level of damping to model the Helmholtz resonator.

REFERENCES

American Society of Civil Engineers, & Structural Engineering Institute. (2005). *Minimum design loads for buildings and other structures / American Society of Civil Engineers.* Reston, VA: American Society of Civil Engineers, Structural Engineering Institute.

American Society of Civil Engineers, & Structural Engineering Institute. (2010). *Minimum design loads for buildings and other structures / American Society of Civil Engineers.* Reston, VA: American Society of Civil Engineers, Structural Engineering Institute.

Ginger, J., Henderson, D., Edwards, M., & Holmes, J. (2010). *Housing damage in windstorms and mitigation for Australia.* Paper presented at the Wind-Related Disaster Risk Reduction (WRDRR) Activities in Asia-Pacific Region and Cooperative Actions, Inchon, Korea. IAWE Secretariat.

Ginger, J. D., & Holmes, J. D. (2003). Effect of building length on wind loads on low-rise buildings with a steep roof pitch. *Journal of Wind Engineering and Industrial Aerodynamics, 91*(11), 1377-1400

Ginger, J. D., Holmes, J. D., & Kim, P. Y. (2010). Variation of internal pressure with varying sizes of dominant openings and volumes. *Journal of Structural Engineering, 136*(10), 1319-1326

Ginger, J. D., Holmes, J. D., & Kopp, G. A. (2008). Effect of building volume and opening size on fluctuating internal pressure. *Wind & Structures, 11*, 361-376

Hall, W. J., & Wiggins, J. H. (2000). Acceptable Risk: A need for periodic review. *Journal of Natural Hazards Review, 1*(3), 180 - 187

Holmes, J., & Ginger, J. (2012). Internal pressures–The dominant windward opening case–A review. *Journal of Wind Engineering and Industrial Aerodynamics, 100*(1), 70-76

Holmes, J. D. (1994). Wind pressures on tropical housing. *Journal of Wind Engineering and Industrial Aerodynamics, 53*(1), 105-123

Holmes, J. D. (2001). *Wind loading of structures*. Melbourne: Spon Press.

Holmes, J. D., & Ginger, J. D. (2009). *Codification of internal pressures for building design*. Proc., 7th Asia Pacific Conf. on Wind Engineering, Chinese Taiwan Association for Wind Engineering, Taipei, Taiwan.

National Hurricane Center (2009). *Atlantic Best Tracks, 1851 to 2008*. National Oceanic and Atmospheric Administration.

U.S. National Oceanic and Atmospheric Administration (1974, December 25). *Tropical cyclone records*. Retrived from http://www.ntlib.nt.gov.au/tracy/advanced/Met/25am.html

U.S. National Oceanic and Atmospheric Administration (1979, October 12). *Faq : hurricanes, typhoons, and tropical cyclones*. Retrived from http://www.aoml.noaa.gov/hrd/tcfaq/E5.html

Jenkinson, A. F. (1955). The frequency distribution of the annual maximum (or minimum) values of meteorological elements. *Quarterly Journal of the Royal Meteorological Society, 81*(348), 158-171

Wehner, M., Ginger, J., Holmes, J., Sandland, C., & Edwards, M. (2010). *Development of methods for assessing the vulnerability of Australian residential building stock to severe wind.* Paper presented at the IOP Conference Series: Earth and Environmental Science. IOP Publishing: 1 pg. (012017)